Comparative distribution of Neuropeptide Y Y1 and Y5 receptors in the rat brain by using immunohistochemistry

ARTICLE *in* THE JOURNAL OF COMPARATIVE NEUROLOGY · SEPTEMBER 2003

Impact Factor: 3.23 · DOI: 10.1002/cne.10823 · Source: PubMed

THE JOURNAL OF COMPARATIVE NEUROLOGY 464:285–311 (2003)

Comparative Distribution of Neuropeptide Y Y1 and Y5 Receptors in the Rat Brain by Using Immunohistochemistry

MICHAEL L. WOLAK,[1] M. REGINA DEJOSEPH,[1] ALLISON D. CATOR,[1] ASHWINI S. MOKASHI,[1] MARK S. BROWNFIELD,[2] AND JANICE H. URBAN[1]*
[1]Department of Physiology and Biophysics, Finch University of Health Sciences/Chicago Medical School, North Chicago, Illinois 60064
[2]Department of Comparative Biosciences and Neuroscience Training Program, University of Wisconsin School of Veterinary Medicine, Madison, Wisconsin 53706

ABSTRACT

Neuropeptide Y (NPY) Y1 and Y5 receptor subtypes mediate many of NPY's diverse actions in the central nervous system. The present studies use polyclonal antibodies directed against the Y1 and Y5 receptors to map and compare the relative distribution of these NPY receptor subtypes within the rat brain. Antibody specificity was assessed by using Western analysis, preadsorption of the antibody with peptide, and preimmune serum controls. Immunostaining for the Y1 and Y5 receptor subtypes was present throughout the rostral–caudal aspect of the brain with many regions expressing both subtypes: cerebral cortex, hippocampus, hypothalamus, thalamus, amygdala, and brainstem. Further studies using double-label immunocytochemistry indicate that Y1R immunoreactivity (-ir) and Y5R-ir are colocalized in the cerebral cortex and caudate putamen. Y1 receptor ir was evident in the central amygdala, whereas both Y1- and Y5-immunoreactive cells and fibers were present in the basolateral amygdala. Corresponding with the physiology of NPY in the hypothalamus, both Y1R- and Y5R-ir was present within the paraventricular (PVN), supraoptic, arcuate nuclei, and lateral hypothalamus. In the PVN, Y5R-ir and Y1R-ir were detected in cells and fibers of the parvo- and magnocellular divisions. Intense immunostaining for these receptors was observed within the locus coeruleus, A1–5 and C1–3 nuclei, subnuclei of the trigeminal nerve and nucleus tractus solitarius. These data provide a detailed and comparative mapping of Y1 and Y5 receptor subtypes within cell bodies and nerve fibers in the brain which, together with physiological and electrophysiological studies, provide a better understanding of NPY neural circuitries. J. Comp. Neurol. 464:285–311, 2003.

Indexing terms: NPY; hypothalamus; hippocampus; amygdala

Neuropeptide Y (NPY), peptide YY (PYY), and pancreatic polypeptide (PP) comprise the pancreatic polypeptide family of neuropeptides. NPY is widely distributed in the central (Chronwall et al., 1985; de Quidt and Emson, 1986; Chronwall, 1989) and peripheral (Lundberg et al., 1982) nervous systems and is implicated in the regulation of several physiological processes, including but not limited to food intake (Stanley et al., 1986), blood pressure (Carter et al., 1985), anxiety (Wahlestedt et al., 1993; Kask et al., 1998a), hormone secretions (Wahlestedt et al., 1987; Leibowitz et al., 1988; Bauer-Dantoin et al., 1991), epilepsy (Baraban et al., 1997), circadian rhythms (Biello, 1995), and neuromodulation (Kapoor and Sladek, 2001). Currently, there are at least six receptor subtypes identified for NPY and its family of related ligands: Y1, Y2, Y3, Y4, Y5, Y6. Of these G protein-coupled receptors (GPCR),

Grant sponsor: Grant number: R29 MH53663; Grant sponsor: Schweppe Foundation (J.H.U.); Grant sponsor: Sigma Xi Grant-in-Aid (M.L.W.).

Dr. Michael L. Wolak's current address is Section of Neurosurgery, Dartmouth-Hitchcock Medical Center, Lebanon, NH 03756.

*Correspondence to: Janice H. Urban, Department of Physiology and Biophysics, FUHS/Chicago Medical School, 3333 Green Bay Road, North Chicago, IL 60064. E-mail: urbanj@finchcms.edu

Received 26 August 2002; Revised 3 April 2003; Accepted 9 April 2003
DOI 10.1002/cne.10823
Published online the week of August 4, 2003 in Wiley InterScience (www.interscience.wiley.com).

the Y1, Y2, Y4, and Y5 receptors have been cloned in the rat and human and are associated with Gi proteins, which negatively couple to adenylate cyclase (Eva et al., 1990; Gerald et al., 1995, 1996; Bard et al., 1995). Compared with many of the other GPCR superfamilies, the NPY receptor family has a high degree of sequence conservation among species (with over 93% conservation between rat and human receptor sequences) and, in contrast, has a

Abbreviations

ac	anterior commissure
AD	anterodorsal nucleus, thalamus
AH	anterior hypothalamus
AHP	anterior nucleus, posterior hypothalamus
AM	anteromedial nucleus, thalamus
Amb	ambiguus n.
AP	area postrema
ArcN	arcuate nucleus
ArcL	arcuate nucleus, lateral
ArcM	arcuate nucleus, medial
AStr	amygdalostriatal transition area
B	basal nucleus of Meynert
BLA	basolateral nucleus, anterior, amygdala
BLP	basolateral nucleus, posterior, amygdala
BLV	basolateral nucleus, ventral, amygdala
BM	basomedial nucleus, amygdala
BST	bed nucleus of the stria terminalis
BSTL	bed nucleus of the stria terminalis, lateral
BSTM	bed nucleus of the stria terminalis, medial
CA	cornu Ammon's
Cb	cerebellum
cc	corpus callosum
CC	central canal
CeAm	central amygdala
CeL	central amygdala, lateral
CeM	central amygdala, medial
cir	circular n.
CL	centrolateral thalamic n.
Cl	claustrum
CPu	caudate putamen
cst	commissural stria terminalis
ctx	cerebral cortex
DA	dorsal hypothalamic area
DBB	diagonal band of Broca
DEn	dorsal endopiriform
DG	dentate gyrus
DLG	dorsal lateral geniculate
DMPAG	dorsomedial periaqueductal gray
DR	dorsal raphe
ECIC	external cortex of the inferior colliculus
ECu	external cuneate n.
f	fornix
fmj	forceps major of the corpus callosum
Gi	gigantocellular reticular nucleus
GrDG	granular layer, dentate gyrus
HDB	horizontal limb of the diagonal band
hf	hippocampal fissure
Hip	hippocampus
ic	internal capsule
ICj	island of Calleja
IO	inferior olive nucleus
IP	interpeduncular n.
LaV	lateral nucleus, ventral, amygdala
LC	locus coeruleus
LD	laterodorsal nucleus, thalamus
LG	lateral geniculate
LHA	lateral hypothalamic area
LM	lateral mammillary nucleus
LPB	lateral parabrachial n.
LPGi	lateral paragigantocellular n.
LPLC	lateral posterior thalamic n.
LRt	lateral reticular nucleus
LSD	lateral septal nucleus, dorsal
LSI	lateral septal nucleus, intermediate
LSO	lateral superior olive
MCPO	magnocellular preoptic nucleus
MCPC	magnocellular n. of the posterior commissure
MD	mediodorsal nucleus, thalamus
ME	median eminence
MeAm	medial amygdala
Me5	mesencephalic trigeminal nucleus
MG	medial geniculate
MHb	medial habenula
MM	medial mammillary nucleus, medial
MolDG	molecular layer, dentate gyrus
MPA	medial preoptic area
MR	medial raphe n.
MS	medial septal nucleus
MVe	medial vestibular nucleus
NAc	nucleus accumbens
nts	nucleus tractus solitarius
Op	optic nerve layer of the superior colliculus
or	oriens layer of the hippocampus
ox	optic chiasm
PaDC	paraventricular n., dorsal cap
PaLM	paraventricular n., lateral magnocellular
PaMP	paraventricular n., medial parvocellular
PaV	paraventricular n., ventral
Par2	parietal cortex 2
pc	posterior commissure
PDTg	posterior tegmental nucleus
PeV	periventricular nucleus
PeF	perifornical nucleus
Pir	piriform cortex
PnC	pontin reticular n., caudal part
PnO	pontin reticular n., oral part
Po	posterior thalamic nuclear group
PoDG	polymorphic layer, dentate gyrus
PR	prerubral field
Pr	prepositus n.
Pr5	principal sensory trigeminal n.
PT	parataenial thalamic n.
PVA	paraventricular n., anterior
PVN	paraventricular nucleus
Pu	Purkinje layer, cerebellum
Py	pyramidal layer, hippocampus
Rad	radiatum layer, hippocampus
RCh	retrochiasmatic n.
RE	retrosplenial cortex
Re	reuniens nucleus, thalamus
Rt	reticular nucleus
S	subiculum
SCh	suprachiasmatic nucleus
Sfi	septofimbrial nucleus
sm	stria medullaris
SN	substantia nigra
SNC	substantia nigra, pars compacta
SNR	substantia nigra, pars reticulata
Sol	nucleus of the solitary tract
SolC	nucleus of the solitary tract, common
SolM	nucleus of the solitary tract, medial
SolI	nucleus of the solitary tract, interstitial
SON	supraoptic nucleus
SpVe	spinal vestibular n.
Sp5	spinal trigeminal nucleus
SubC	subcoeruleus
Tz	trapezoid body
VA	ventral anterior nucleus, thalamus
VDB	ventral limb of the diagonal band
VL	ventrolateral nucleus, thalamus
VMH	ventromedial nucleus, hypothalamus
VM	ventromedial nucleus, thalamus
VMHVL	ventromedial hypothalamic n, ventrolateral part
VMHVM	ventromedial hypothalamic n, ventromedial part
VP	ventral pallidum
VPL	ventral posterolateral thalamic n.
VPM	ventral posteromedial thalamic n.

relatively low sequence homology among the different receptor subtypes (31% homology between and Y1 and Y2 receptors and 42% homology exists between the Y1 and Y4 receptors [Larhammar, 1996]). Radioligand studies demonstrate binding sites for NPY and related ligands in the brain, peripheral nervous system, vasculature, and numerous peripheral organs, including heart, adrenal, ovary/testis, and gastrointestinal tract (Allen et al., 1993; Dumont et al., 1993; Ghilardi et al., 1994). Both radioligand and in situ hybridization analyses reveal distinct patterns of distribution for each of these receptors providing anatomic correlates for the physiological role of NPY receptor activation.

Of all the NPY receptors, the Y1 and Y5 receptor (Y1R, Y5R) subtypes have received significant attention based on their ability to increase food intake (Schaffhauser et al., 1997; Duhault et al., 2000), modulate anxiety (Wahlestedt et al., 1993; Heilig et al., 1993), and regulate hormone secretions (Leupen et al., 1997; Hastings et al., 2001). The Y1 receptor was the first receptor to be cloned and is perhaps the best characterized receptor for NPY (Eva et al., 1990, 1992). In situ hybridization reveals the distribution of Y1R mRNA in the brain of several mammalian species, with the highest levels of expression consistently seen in forebrain regions, including the cerebral cortex, the hippocampal formation, and several amygdaloid, thalamic, and hypothalamic nuclei (Mikkelsen and Larsen, 1992; Parker and Herzog, 1999). In addition, high level expression of Y1R mRNA has been detected in numerous brainstem nuclei. Within these brain regions, the Y1 receptor is generally considered to be postsynaptic. However, immunohistochemical studies by Pickel et al. (1998) identified the presence of Y1 receptors in NPY-immunoreactive terminals, which suggests that the Y1R may also be a presynaptic receptor.

The Y5 receptor has been cloned more recently (Gerald et al., 1996). Binding sites as well as mRNA for the Y5R has been found within cerebral cortex, hippocampus, hypothalamus, amygdala, and brainstem nuclei (Dumont et al., 1998a; Durkin et al., 2000). The Y5 receptor has similar actions to the Y1 receptor in that it regulates or modulates food intake (Marsh et al., 1998), anxiety (Sajdyk et al., 2002), and γ-aminobutyric acid (GABA) release (Pronchuk et al., 2002). Y1 and Y5 receptor mRNA have very similar patterns of distribution and, because these receptors have overlapping gene structures, it has been postulated that there is coordinated expression of Y1 and Y5 receptors (Herzog et al., 1997). Whereas data demonstrates overlap of the distribution of the Y1 and Y5 receptors, it remains to be determined whether these receptors are expressed in the same cell. Further examination of the distribution and coexpression of these receptors in individual cells will be instrumental in determining the degree of participation of each of these receptors in physiological processes.

The present studies were designed to examine the localization and distribution of the Y1 and Y5 receptors in the rat brain by using single- and double-label immunohistochemistry. In several sites within the brain, NPY exerts potent physiological effects (i.e., feeding effects in the PVN), yet there is minimal ligand binding in these areas as detected by means of receptor autoradiography. Using immunocytochemistry affords higher sensitivity to detect individual cells and/or fibers with low levels of receptor expression. Comparing the distribution and cellular localization of these receptors provides more information regarding the role of these receptors in regulating physiology and an additional, and complementary, way of examining NPY receptor localization.

MATERIALS AND METHODS

Animals

Adult male Sprague-Dawley rats (Charles River; 250–350 g) were maintained under standardized lighting conditions (14:10 light:dark cycle) in a temperature-controlled environment (23°C) with free access to rat chow and tap water. All procedures were approved by the institutional animal care and use committee (IACUC).

For tissue fixation, animals were anesthetized with an intraperitoneal (i.p.) injection of sodium pentobarbital (Anpro Pharmaceutical; 50 mg/kg) and transcardially perfused with 25 ml of phosphate-buffered saline (PBS: 10 mM Na_2HPO_4, 150 mM NaCl, pH 7.5) containing 0.1% procaine and 100 U/ml heparin at 37°C followed by 50 ml of fixative solution (4% paraformaldehyde in PBS [pH 8.0]) at +4°C. Brains were rapidly dissected out, post-fixed for 18–24 hours in fixative solution at +4°C, and stored in PBS (pH 7.5) at +4°C. Coronal brain sections were cut at 30–40 μm thicknesses on a Vibratome, and free-floating sections were collected in ice-cold PBS (pH 7.5) and processed for immunohistochemical staining.

Y1 and Y5 Antisera

Polyclonal Y1R and Y5R antisera were generated in rabbits. The selection of the targeted peptide sequences was based on computer analysis of the full-length Y1R and Y5R sequences listed in the Swiss Protein Database using GeneRunner (Hastings Software, Hastings on Hudson, NY) and Peptide Structure Genetics Computer Group (GCG, Madison, WI) software. The peptides were selected based on high antigenicity, surface probability, and surface topology indices. A C-terminal peptide consisting of amino acids 363-382 of the NPY Y1 receptor was synthesized (Quality Control Biochemicals; LKQASPVAFKKISMNDNEKI), conjugated to keyhole limpet hemocyanin (KLH), and injected into rabbits (initially with 500 μg and subsequently with 50-μg boosts once per month for 18 months). Similarly, a peptide corresponding to extracellular loop 3 and parts of transmembrane domains VI/VII of the NPY Y5 receptor was synthesized (VTDFNDNLISNRHFKLVYCIC; representing amino acids 400-420), conjugated to KLH and injected into rabbits. Rabbits were bled 10 days after each immunogen injection, plasma was collected and affinity purified. Purified antibody was prepared by affinity chromatography against immobilized rat Y1R(363-382) or Y5R(400-420) medium prepared by using a Pierce SulfoLink kit (Rockford, IL). Antibodies were eluted with 0.2 M glycine (pH 2.5) and collected into 1.0 M Tris (pH 8.0). Antisera were extensively dialyzed against PBS and made up in 1% bovine serum albumin (BSA) and 0.01% sodium azide. No similarity between the synthetic peptides and the sequence of other currently cloned NPY receptor subtypes or other transmembrane receptors has been found in searches against updated databanks (Nonredundant GenBank CNS). The specificity of each antiserum was assessed with Western analysis, immunohistochemistry using preimmune sera and preadsorption of the antibody with the synthetic peptides used to generate

the respective antisera in rabbit at a concentration ratio of 1:10 (antiserum:peptide).

Immunocytochemistry

Free-floating sections were washed in immunocytochemistry (ICC) buffer consisting of 0.2% gelatin, 0.01% thimerosal, 0.002% neomycin in PBS (pH 7.5), blocked with antibody dilution buffer (ICC buffer containing 2% normal goat serum [NGS; Vector Laboratories]) for 30 minutes at +4°C, and then incubated for 24–48 hours at +4°C with either the rabbit anti-Y1 receptor antiserum (1:2,000) or rabbit anti-Y5 receptor antiserum (1:20) diluted in ICC buffer with 2% NGS. Sections were washed in ICC buffer and then incubated for 45 minutes at room temperature with biotinylated, affinity purified goat anti-rabbit IgG (H+L; Vector Laboratories; 1:400), followed by a wash in ICC buffer and incubation for 45 minutes at room temperature with an avidin-biotin-horseradish peroxidase (ABC) complex (VECTASTAIN *Elite* ABC, Vector Laboratories; 1:300). Sections were washed in Tris-buffered saline (TBS: 100 mM Tris base, 150 mM NaCl, pH 7.5), and signal was developed by incubating sections in a chromogenic substrate solution consisting of 0.03% 3,3′-diaminobenzidine (DAB), 0.01% H_2O_2, and 0.03% $NiCl_2$ in TBS (pH 7.5). Color development was carefully monitored and proceeded at room temperature for 10–15 minutes, after which time the sections were washed in TBS and mounted on gelatin-coated slides. Mounted sections were dehydrated in a series of ascending ethanol washes (50, 70, 80, 90, 100, 100%) and cleared in a xylene substitute (Hemo-De; Fisher). Coverslips were applied with Permount.

Brain sections were atlas matched according to the stereotaxic rat atlas of Paxinos and Watson (1997), and immunoreactive staining was visualized by light microscopy. The distribution of Y1R immunoreactivity (-ir) and Y5R-ir presented in the table was determined in sections from 10 animals. Specific signal, in part, was assessed in alternate sections incubated with antibody that was preincubated with immunizing peptide. The distribution and degree of immunostaining for each antibody in each brain region was assessed by two different investigators. By using a predetermined scale, the cell density and relative intensity (Fig. 1) of signal was rated. Images were captured by using a SPOT 2 digital camera and MetaMorph software; the contrast and brightness of the photomicrographs were adjusted by using MetaMorph software or Adobe Photoshop. Montages were assembled by using Adobe Photoshop.

Double-label immunocytochemistry

To assess colocalization of Y1 and Y5 receptors in the same cell, we used a standard secondary antibody immunofluorescence protocol combined with biotinylated tyramide amplification immunofluorescence based on that described by Adams (1992). As both the Y1 and Y5 antisera were generated in rabbits, there were technologic concerns regarding the generation of false positives in the double-label immunocytochemical assays. Using biotinylated tyramide to enhance the detection of one antibody allowed us to use one antiserum at dilutions below the limit of detectability using standard secondary antibody immunofluorescence methods. Briefly, tissues were incubated with one antibody (Y1 or Y5 receptor), visualized by using the biotinylated tyramide enhancement and then

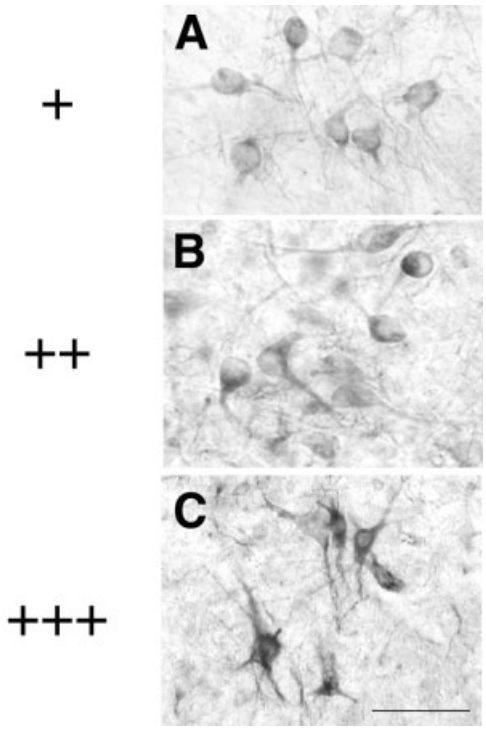

Fig. 1. Representative cells for the different labeling intensity rankings (+, ++, +++) indicated in Table 1. **A:** Y1R-labeled cells in the ventral pallidum. **B:** Y1 receptor (Y1R) -labeled cells in the dorsal hypothalamus. **C:** Y5R-labeled cells in the locus coeruleus. Scale bars = 50 μm in C (applies to A–C).

processed for the other NPY receptor subtype by using standard secondary antibody immunofluorescence histochemistry. Brains (n = 5) were processed as mentioned above and free-floating sections were washed in PBS followed by incubation in 1% H_2O_2 for 15 minutes and 3% normal donkey serum in antibody dilution buffer for 30 minutes at room temperature. The sections were incubated with primary antibody (Y1, 1:3,000; Y5, 1:100) for 36–48 hours at +4°C. The sections were washed in ICC buffer (5 × 5 minutes) and incubated in biotinylated donkey anti-rabbit (1:2,500) for 1 hour at room temperature. After rinses in ICC buffer, the sections were incubated in ABC complex (VECTASTAIN *Elite* ABC; 1.5 μl/ml) for 30 minutes, rinsed with PBS (5 × 5 minutes), and incubated with biotinylated tyramide (1.5 μl/ml) for 10 minutes at room temperature. Tissues were washed in PBS (5 × 5 minutes) and incubated with either Cy2- or Cy3-conjugated strepavidin (1:250) for 3 hours. After PBS washes (5 × 5 minutes), the sections were incubated with the second primary antiserum (Y1:1:800; Y5: 1:20) for 36–48 hours at +4°C. After another series of PBS washes (5 × 5 minutes) the sections were incubated with Cy2- or Cy3-conjugated donkey anti-rabbit antisera (1:250). The tissues were rinsed in PBS (5 × 5 minutes), mounted on gelatin-coated slides, and allowed to air-dry. Coverslips were applied by using 2.5% PVA-DABCO (polyvinyl alcohol; 1,4-diazabicyclo[2.2.2]octane) antifade mounting medium.

Immunocytochemical staining was visualized by using an Olympus Fluoview Scanning Laser confocal micro-

scope. Images were obtained by using the Fluoview software, and contrast was optimized by using Adobe Photoshop. The specificity of the signal was assessed by omission of either one or the other antibody through the double-label protocol and peptide preadsorption of each antibody. Both antibodies were titrated by using both immunofluorescence procedures to characterize the staining patterns and ensure that no nonspecific staining was generated in the double-label procedure. Additionally, the overall distribution of Y1R-ir and Y5R-ir was not different than that presented in Table 1, although the signals were more intense.

Cell culture

The human neuroblastoma cell line SK-N-MC, which expresses the Y1 receptor subtype, was obtained from the American Type Culture Collection (ATCC; Rockville, MD). Cells were grown in Eagle's Minimum Essential Medium (EMEM; Gibco-BRL) supplemented with 10% fetal bovine serum, 1.0 mM sodium pyruvate, 50 U/ml penicillin, and 25 μg/ml streptomycin. Cells were maintained in a water-saturated atmosphere of 95%O_2/5% CO_2 at 37°C and grown to 70% confluence. At the third to fifth passage, cells were rinsed in TBS supplemented with 1 mM EDTA (pH 8.0) and protease inhibitors (Boehringer *Complete* protease inhibitor tablets), harvested, pelleted by brief centrifugation, and stored at −80°C.

Sodium dodecyl sulfate-polyacrylamide gel electrophoresis and Western analysis of rat brain homogenate and SK-N-MC cells

Brains were rapidly dissected out and homogenized (Polytron homogenizer; Brinkmann Instruments) in Tris buffer supplemented with 1 mM EDTA (pH 8.0) and protease inhibitors. The homogenates were centrifuged (15,000 × *g* for 20 minutes), and the resulting supernatant was stored at −80°C. For preparation of membrane- and cytosol-enriched fractions, tissue was homogenized and centrifuged (1,000 × *g* for 10 minutes). The supernatant containing solubilized receptor was further centrifuged at 100,000 × *g* for 1 hour at 4°C. The supernatant containing the cytosol-enriched fractions (S100) was collected, and the pellet containing the membrane-enriched fraction (P100) was resuspended in sodium dodecyl sulfate-polyacrylamide gel electrophoresis (SDS-PAGE) buffer and subsequently stored at −80°C.

Homogenates of brain and SK-N-MC cells were diluted in SDS-PAGE sample buffer (60 mM Tris-HCl [pH 6.8], 10% glycerol, 2% SDS, 0.0025% bromophenol blue). Samples containing 50–100 μg of total protein were heated to 90°C for 5 minutes, loaded on 10% Tris-glycine gels in Towbin buffer (24 mM Tris base, 192 mM glycine, pH 8.3) with 0.1% SDS, and separated by electrophoresis (2 hours at 110 V [constant]). Separated proteins were blotted onto polyvinylidene difluoride membranes by electrophoresis (90 minutes at 25 V [constant]) in 0.5× Towbin buffer with 20% methanol and 0.025% SDS. SDS-PAGE and protein transfer were carried out by using the Novex XCell II Mini-Cell apparatus and Blot Module. Immunodetection was performed by using the Novex WesternBreeze chemiluminescent detection system according to manufacturer's instruction, with primary antibody dilutions of 1:2,000 (anti-Y1R antiserum) and 1:30 (anti-Y5R antiserum). Immunoreactive bands were detected by exposure to Kodak X-OMAT AR film at room temperature for 5–15 minutes, and molecular weights were estimated by using Bio-Rad Kaleidoscope and SeaBlue prestained standards. Specificity controls were performed by preincubation of the anti-Y1R and anti-Y5R antisera with the peptides used to generate the respective antisera.

RESULTS

The distribution of Y1R-ir and Y5R-ir extends throughout the rostral–caudal extent of the brain with Y1R overall being more widely distributed than Y5R. Both receptors were present with relatively high concentrations of cell bodies and fibers within the cortex, hippocampus, hypothalamus, amygdala, and brainstem corresponding with some of the major actions of NPY. Figure 2 is a diagrammatic representation of the distribution of cell body (dots/triangles) and fiber (stippled areas) density for Y1R-ir (left side of diagram) and Y5R-ir (right side of diagram). The information presented in Table 1 indicates the relative density of Y1R- and Y5R-containing cells within a region and the intensity of immunoreactivity in these different brain regions. The relative labeling intensities of cells and fibers were assessed by using the scale represented in Figure 1. A (+) was given to those cells and fibers that exhibited a light, uniform immunostaining (Fig. 1A). The presence of a darker immunostaining pattern or a variation in labeling intensity was represented as ++ (Fig. 1B). In some cases, the staining was very intense (black); this staining was represented with +++ (Fig. 1C). That we observe differences in signal intensities among brain regions suggests that the current staining condition has a dynamic range which allows for detection of differential receptor expression under physiological conditions. Immunoreactive staining was absent in those sections incubated with preimmune serum or antisera that was preincubated with peptide sequences used to generate the antibodies (Fig. 3).

Western analysis of SK-N-MC cells (Fig. 4) revealed a single band migrating at approximately 42 kDa, which is in agreement with the predicted molecular weight of the Y1 receptor protein (Eva et al., 1990). In Western blots of brain homogenates, two specific immunoreactive bands for the Y1 receptor were identified: a light band at 42 kDa and a band at ~85 kDa. These bands showed a differential distribution when compared in membrane-enriched (P100) vs. cytosol-enriched (S100) protein fractions. In membrane-enriched (P100) fractions, two bands were present that corresponded to ~42 and ~85 kDa, whereas the lower molecular weight species was not present in the cytosol-enriched fraction (S100). For the Y5 receptor, Western blots of rat brain homogenates revealed two bands migrating at ~45–50 kDa, corresponding to the predicted molecular weight of the Y5 receptor protein (Gerald et al., 1996). The presence of these bands was abolished in preadsorption control assays. No Y5R-immunoreactive band was present in homogenates from the SK-N-MC cells.

Telencephalon

Within the neocortex, the strongest labeling of Y1R-ir perikarya was localized to a cluster of neurons present in layers IV/V of parietal cortex 2 (Par2; Fig. 5A,C). Cell bodies comprising this neuronal population typically displayed long, tapering processes of either a bipolar or multipolar arrangement and were distributed with a low to

TABLE 1. Regional Distribution of Y1 and Y5 Immunoreactivity Throughout the Rostrocaudal Extent of the Brain[1]

Region	Y1 receptor		Y5 receptor	
	Cell density	Staining intensity	Cell density	Staining intensity
Telencephalon				
Neocortex	+/++	+/++	++	++/+++
Periallo- and proisocortex	+/++	+/++	++	++/+++
Dorsal endopiriform cortex	++	++	+	+
Hippocampal formation				
CA1	+++	+	+++	++
CA2	+++	+/++	+++	++
CA3	+++	++/+++	+++	++
Dentate gyrus				
Granule layer (GrDG)	nd	nd	+++	+/++
Molecular layer (MolDG)	fibers	++	fibers	++
Polymorphic layer (PoDG)	++	++/+++	+	++
Subiculum (S)	++	++	++	++
Basal nuclei				
Caudate-putamen (CPu)	+	++	++	++
Nucleus Accumbens (Acb)-shell	+/++	+	++	+
Islands of Calleja (LCJ)	++/+++	++	++	++
Pallidal complex				
Globus pallidus (GP)	+	+	nd	nd
Entopenduncular nucleus (EP)	+	++	+	+
Ventral pallidum (VP)	+/++	++	nd	nd
Claustrum (Cl)	+++	+++	+	+
Basal nucleus of Meynert (B)	+	+++	nd	nd
Septum				
Medial septum-diagonal band (MSDB)	+/++	+/++	+	+
Lateral septum (LS)	+	+	+/++	+
Septofimbrial nucleus (Sfi)	++	+++	+	+++
Amygdaloid complex				
Nucleus of the lateral olfactory tract (LOT)	++/+++	++	nd	nd
Bed n. accessory olfactory tract (BAOT)	+/++	+	nd	nd
Basolateral complex				
Lateral nucleus (La)	+/++	+/++	++	+
Basolateral nucleus (BL)	++/+++	++	++	+
Extended amygdala				
Bed n. stria terminalis-medial (BSTM)	++	++	nd	nd
-lateral (BSTL)	++	+/++	nd	nd
Medial nucleus (Me)	+	+	nd	nd
Central nucleus (Ce)	+/++	++	+	+
Interstitial n. post. limb ant. commissure (IPAC)	+	+/++	nd	nd
Intercalated cell masses (I)	++	++	nd	nd
Bed N. of the anterior commissure (BAC)	+/++	+	nd	nd
Diencephalon				
Thalamus				
Anterior nuclear group				
Anterodorsal nucleus (AD)	++	++	+	+
Anteromedial n. ventral (AMV)	++/+++	++/+++	++	++
Mediodorsal nucleus (MD)	+/++	+/++	++	++
Ventral nuclear group				
Ventromedial n. (VM)	++	++	+	++
Ventrolateral n. (VL)	++	++	+++	++
Ventroanterior n. (VA)	++	++	++	+++
Ventroposterior nuclear complex (VPL/VPM)	+	+/++	++	+/++
Submedius n.-ventral (SubV)	+	+	++	++
Lateral nuclear group				
Lateroposterior n. (LP)	+/++	++	++	+
Laterodorsal n. (LD)-ventrolateral (LDVL)	++	+/++	+	+
-dorsomedial (LDDM)	+	+	+	+
Posterior nuclear group (Po)	++	+	++	++
Intralaminar nuclear group				
Paracentral n. (PC)	+/++	+	nd	nd
Parafascicular n. (PF)	++	++	nd	fibers
Dorsal midline nuclear group				
Paratenial n. (PT)	++/+++	++/+++	++	+++
Interanteromedial n. (IAM)	+/++	+/++	+	+
Reuniens n (Re)	++/+++	++/+++	nd	nd
Subparafasicular n. (SPF)	++	+	nd	nd
Reticular n. (Rt)	++	+/++	++	++/+++
Metathalamus				
Lateral geniculate (LG)-dorsal (DLG)	+/++	+	++	+
Medial geniculate (MG)	+	+/++	++	+/++
Epithalamus				
Medial habenula (Mhb)	+++	+	+++	++
Medial–lateral junction	++	++/+++	nd	nd
Hypothalamus				
Preoptic region				
Anteroventral periventricular n. (AVPe)	++	++	++	++
Magnocellular preoptic n. (MCPO)	++	++	nd	nd
Medial preoptic area (MPA)	+	+/++	+	+
Medial preoptic n. (MPO)	+/++	+/++	+	+
Median preoptic n. (MnPO)	+/++	+/++	nd	nd
Medial preoptic n. (MPO)				
Periventricular preoptic n. (PePO)	+/++	++/+++	nd	nd
Medial preoptic area (MPA)				
Ventromedial preoptic n. (VMPO)	++	++	nd	nd

TABLE 1. (continued)

Region	Y1 receptor		Y5 receptor	
	Cell density	Staining intensity	Cell density	Staining intensity
Anterior region				
Anterior hypothalamic n.-posterior (AHP)	++	+/++	nd	nd
Anterior periventricular n. (PeA)	+/++	++/+++	nd	nd
Lateral hypothalamic area (LH)	+/++	++	+/++	++
Lateroanterior hypothalamic n. (LA)	+/++	+/++	nd	nd
Paraventricular n. (Pa)				
Lateral and medial magnocellular	+++	++	++	++
Parvocellular (medial, anterior, dorsal cap)	++	++/+++	++	+/++
Accessory magnocellular neurons	+++	++	++	+/++
Retrochaismatic n. (Rch)	++	+++	+	+
Stigmoid n.	++	+/++	nd	nd
Suprachiasmatic n. (SCh)	++	+/++	++	+/++
Supraoptic n. (SON)	+++	++	++	++
Ventrolateral n. (VLH)	++	+	nd	nd
Tuberal region				
Arcuate n. (ArcN)				
Dorsal (ArcD)	+	+++	+	++
Medial and lateral (ArcM; ArcL)	++	+++	+	++
Dorsal area (DA)	+	++	+	++
Perifornical area (PeF)	++/+++	++	nd	nd
Subincertal n. (Sl)	+/++	++	nd	nd
Ventromedial hypothalamus-anterior (VMHA)	+/++	+	fibers	+
Mammillary region				
Tuberomammillary n. (TM)	+++	+	++	++
Posterior periventricular n. (PeP)	+/++	++/+++	nd	nd
Mesencephalon				
Substantia nigra (SN)-compacta (SNC)	++	++	+	+
-reticulata (SNR)	+	++	nd	nd
Ventral tegmental area (VTA)	++	++	nd	nd
Red n. (R)-magnocellular (RMC)	++	++	+	++
Medial accessory oculomotor n. (ME3)	++	++	nd	nd
Periaqueductal gray, dorsomedial (DMPAG)	+	++/+++	nd	nd
Dorsal raphe n. (DR)	++	++	+	++
Sphenoid n. (Sph)	+/++	+/++	nd	nd
Trapezoid body (TZ)	++/+++	++	+++	++
Metencephalon/myelencephalon				
Median raphe n. (MR)	++	++	+	++
Locus coeruleus (LC)–subcoeruleus (SubC)	+++	++/+++	+++	+++
Gigantocellular reticular n. (Gi)	+/++	+	+	+
Pontine reticular n. caudal (PnC)	+/++	++	+	+
Lateral reticular n. (Lrt)	++	++	+	++
Inferior olive complex (IO)	++	+/++	+	++
Mesencephalic trigeminal n. (Me5)	++	+++	++	++/+++
Motor trigeminal n. (Mo5)	++	+++	++	++/+++
Spinal trigeminal n. (Sp5)	++	++	+	+
Dorsal motor n. of the vagus (10)	++	++	++	++
Hypoglossal n. (12)	++	++	++	++
Nucleus of the solitary tract	+	++	++	++
Cerebellum (Purkinje layer)	++	+	++	++
Facial n.	nd	nd	+	+
Vestibular n. lateral and medial	+	++	+	++
Raphe magnus	nd	nd	+	++
N. Ambiguus	++	++	++	+++
Lateral paragigantocell (LPGi)	nd	nd	+	+++
Cuneate	++	+	++	++

[1]Cell density and staining intensity was compared for each receptor subtype in representative atlas matched sections and recorded (high, +++; moderate, ++; low, +; and not detected, nd; Cell density represents the relative number of cells within the region, whereas staining intensity reflects the intensity of the signal per cell (see Fig. 1).

moderate density of immunopositive fibers. Y1R-labeled perikarya were also observed throughout several neocortical fields, most consistently within layers II, IV/V, and VIb, as well as in various transition layers of peri- and proisoallocortical fields.

Immunoreactive staining for the Y5 receptor was also observed throughout several cortical fields. The highest cell densities were seen in the cingulate, retrosplenial, frontal, and parietal cortices and were localized primarily to isocortical layers IV/V and corresponding transition layers of the periallo- and proisocortices (Fig. 5B,D). In these regions, medium, oval- to pyramidal-shaped cell bodies, often exhibiting prominent apical processes, were interspersed among a moderate density of immunopositive fibers that extended throughout all the cortical layers. To further extend these studies, double-label immunohistochemistry demonstrated colocalization of Y1 and Y5 receptor immunoreactivities in the retrosplenial cortex (Fig. 6) as well as in parietal cortex. In the retrosplenial/cingulate cortex, there was considerable colocalization of Y1R-ir and Y5R-ir (Fig. 6C, arrows), and single-labeled Y1R but not Y5R cells were also observed (Fig. 6C, arrowheads). Also note the high degree of Y1R and Y5R fiber staining that appears in a continuum along the apical processes.

Several populations of Y1R-ir perikarya were observed throughout the major divisions of the hippocampal formation (Fig. 7A). Within the dentate gyrus, small to medium immunoreactive cell bodies having short processes with a predominantly bipolar arrangement were localized to the hilus, or polymorphic layer (Fig. 7C), whereas the granule cells had little detectable Y1R-ir. The largest and most densely distributed population of Y1R-labeled perikarya in the hippocampal formation was observed within the

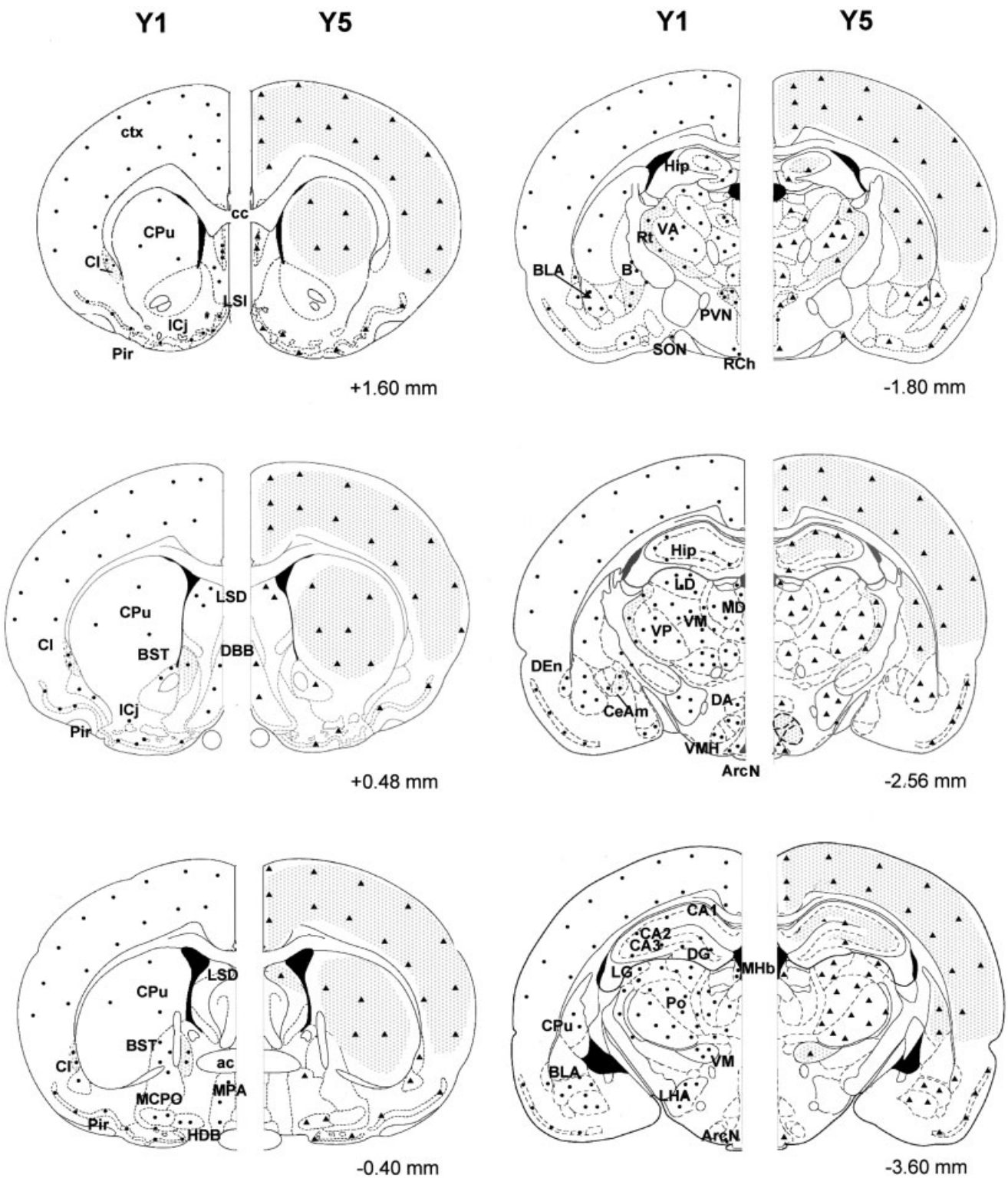

Fig. 2. Diagrammatic representation and comparison of Y1 receptor (Y1R; left) and Y5R (right) immunoreactivity in coronal sections though an adult male rat brain. The coronal sections, with reference to bregma, correspond to the stereotaxic atlas of Paxinos and Watson (1997). The diagrams illustrate the relative distribution of immunopositive cell bodies (Y1R, black dots; Y5R, black triangles) and immunoreactive fibers (represented by stippling). The number of dots/triangles within an area reflects the relative area of distribution and not quantitation of cell number or density. For abbreviations, see list.

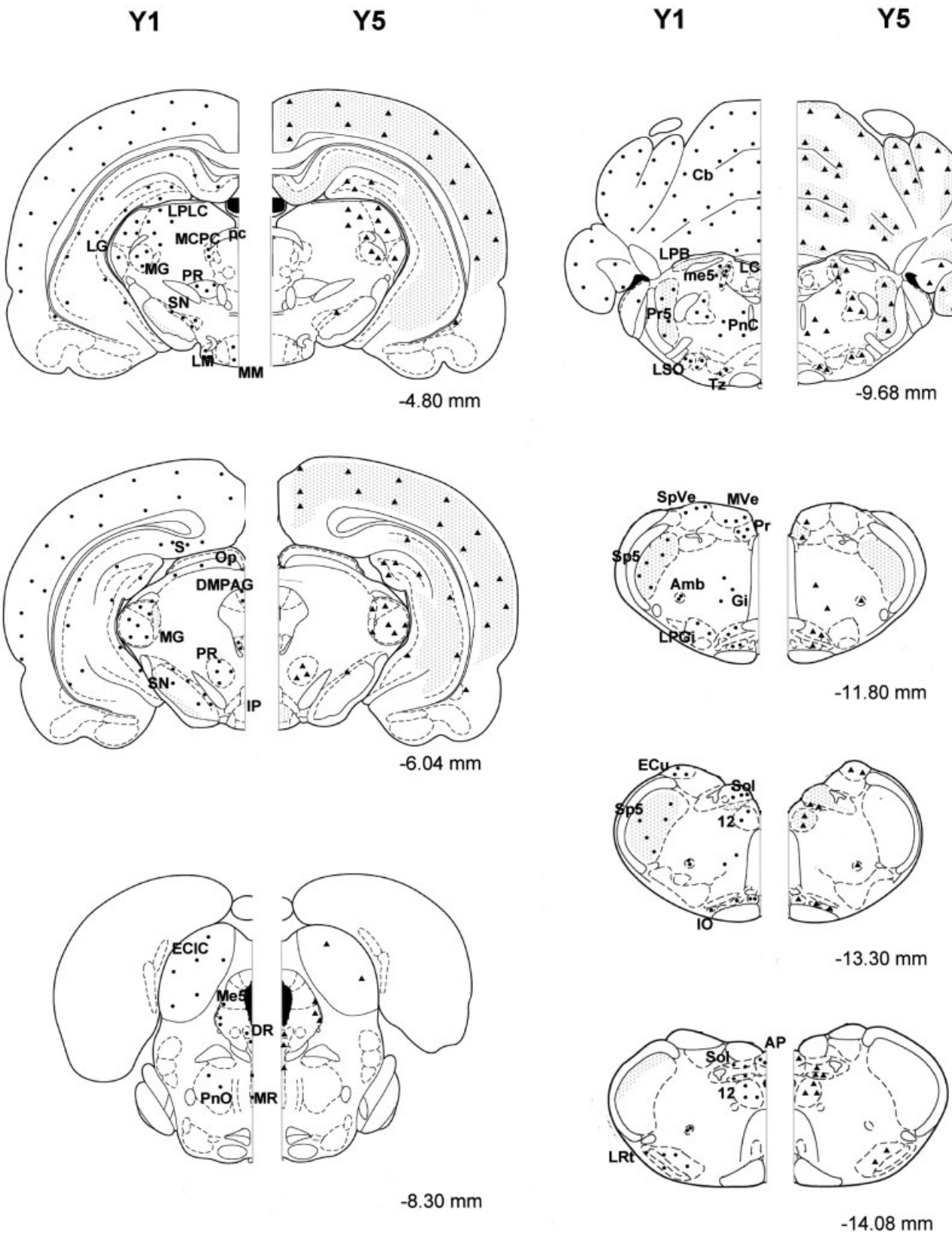

Figure 2 (Continued)

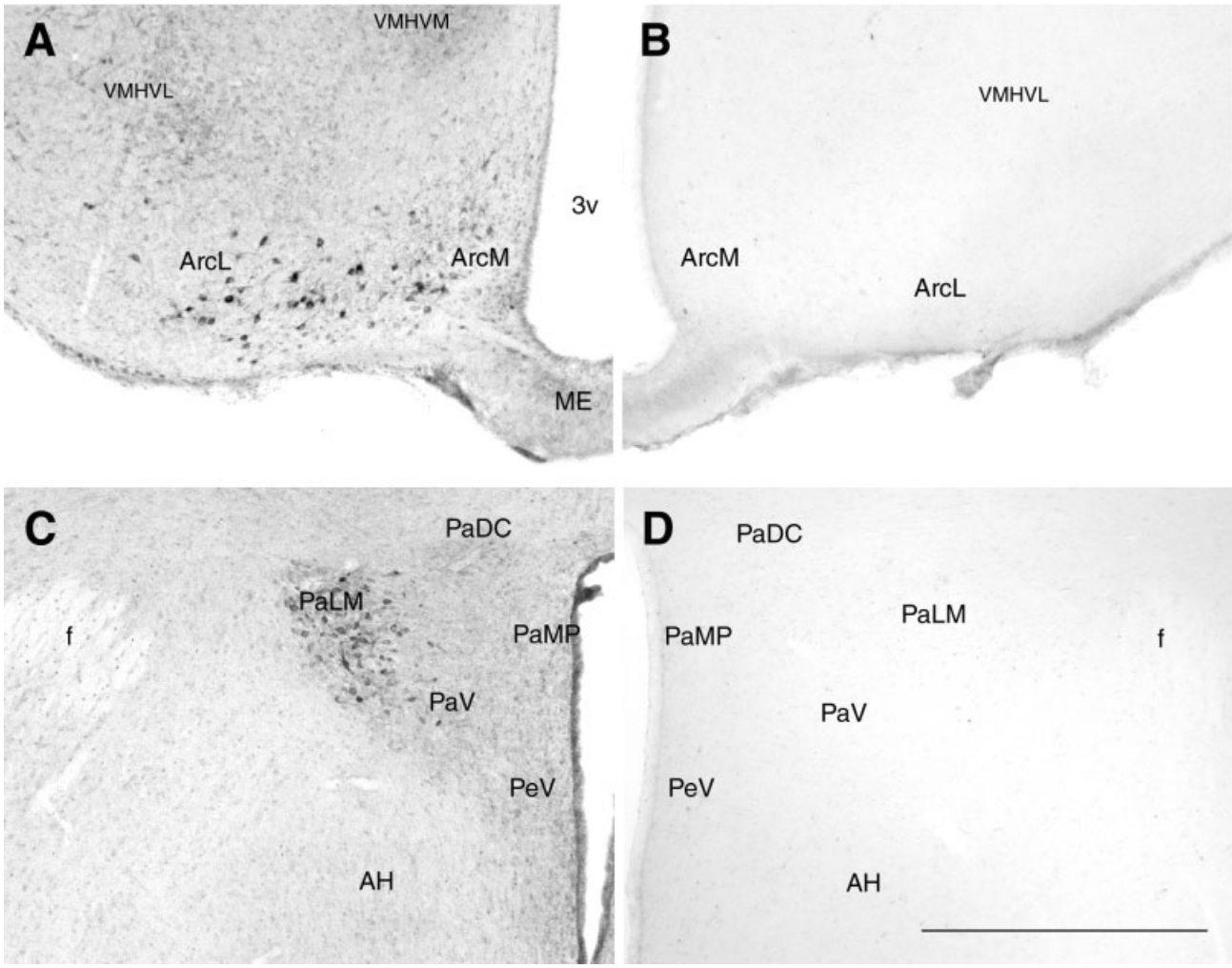

Fig. 3. Specificity of Y1 receptor (Y1R) and Y5R immunostaining. Photomicrographs of Y1R immunostaining in the ArcN (**A**) and Y5 receptor immunostaining in the PVN (**C**) from a male rat. **B,D:** The lack of a specific signal in corresponding sections after preadsorption of the antibodies with the peptide used to generated the respective antiserum. For abbreviations, see list. Scale bars = 500 μm in D (applies to A–D).

stratum pyramidale of Ammon's horn (CA2 and CA3; Fig. 7A). This population of pyramidal-shaped cell bodies were moderately labeled and characteristically displayed short, tapering apical processes oriented perpendicular to the adjacent stratum radiatum. The subiculum contained a moderate to high density of predominantly pyramidal-shaped Y1R-immunoreactive cell bodies displaying short apical processes (Fig. 7F). A low-density of Y1R-immunoreactive fibers was localized predominantly to the oriens, pyramidal, and radiatum strata of Ammon's horn (CA1, CA2, and CA3). Several of these fibers were emanating off of cell bodies in these regions, whereas dense Y1R-immunoreactive staining was present on fine fibers in the MolDG. Also prominent within the hippocampal formation were Y1R-ir perikarya randomly distributed throughout the various strata of Ammon's horn (CA1, CA2, and CA3; Fig. 7D). These cells were medium to large in size and characteristically displayed a multipolar arrangement of arborizing processes. These processes were predominantly oriented perpendicular to the hippocampal fissure and could often be traced for several micrometers.

Y5R-immunoreactive perikarya were also abundantly observed throughout the hippocampal formation. Y5R-ir fibers were observed projecting from cells within the CA1–3 regions (Fig. 7B) and extended into the corresponding stratum radiatum. In general, both the distribution and morphology of Y5R-labeled neurons closely matched the immunoreactive staining patterns observed for the Y1R receptor, with the pyramidal cell layer and the polymorphic dentate gyrus (Fig. 7E,G) showing the highest levels of immunoreactivity. There was colocalization of Y1R-ir and Y5R-ir in cells of the CA1–3 regions with approximately 50% of Y1R-immunopositive cells showing colocalization with the Y5R. This percentage is a conservative estimate of cell number as Y1R and Y5R is differentially expressed in the stratum pyramidale. In general, Y5R-ir is stronger on fibers and proximal dendrites, whereas Y1R-ir is present mostly on cell bodies. Strong

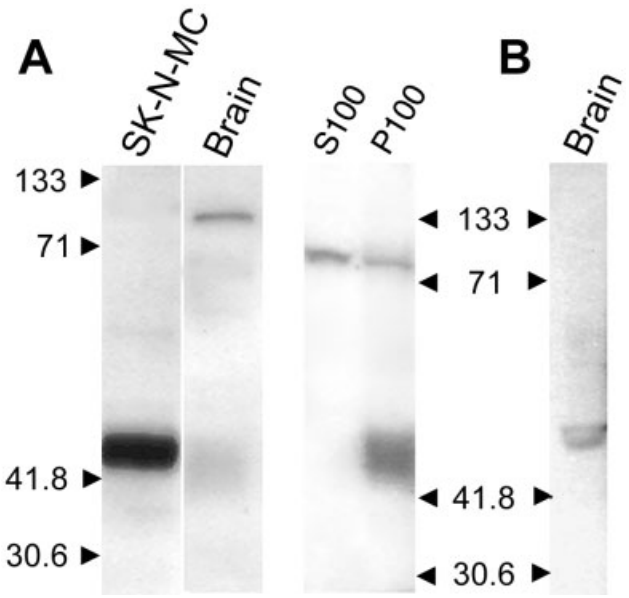

Fig. 4. Western blot analysis of (A) Y1 receptor (Y1R) and (B) Y5R immunoreactivity in rat brain and SK-N-MC cells. **A:** Y1R immunoreactivity in protein homogenates from SK-N-MC cells, brain, and cytosol-enriched (S100) and membrane-enriched (P100) fractions from rat brain. **B:** Immunoblot showing Y5R immunoreactivity in whole brain tissue. Molecular weight markers (kilodaltons) are indicated on the left side of the diagram and between A and B.

Y5R-ir was also evident on cells interspersed throughout the stratum pyramidale similar to that identified in Figure 7D, although they were much fewer in number than the Y1R-ir cells. No colocalization of Y1R- and Y5R-ir was found in these cells.

In septal areas, a prominent cluster of Y1R-immunoreactive perikarya and fibers was observed in the rostral portion of the septofimbrial nucleus (Fig. 8E). This neuronal population displayed an intermediate density of cell bodies with extensive processes, the latter of which contributed to a dense fiber plexus that could be seen projecting ventrally within the precommissural fornix. The Y5R also showed strong immunoreactive staining within this region, although there were fewer cell bodies present. Both Y1R- and Y5R-immunoreactive perikarya were present in the medial septum-diagonal band complex (Fig. 8A,B) with generally more cells showing labeling for Y1R (Fig. 8C) than Y5R (Fig. 8D).

Y1R- and Y5R-immunoreactive perikarya were identified in several telencephalic components of the basal nuclei, including the caudate putamen (CPu; Fig. 9A–C), accumbens nucleus (NAc), olfactory tubercle, and pallidal complex (Fig. 1A). Within the CPu, there was considerable colocalization of the two receptor subtypes (Fig. 9C). Analysis of sections from different animals suggests that ~98% of Y1R-immunoreactive cells are colocalized with Y5R; there are populations of Y5R-ir cells (approximately 35%) that do not coexpress Y1R (Fig. 9C, arrowheads). Outside the corpus striatum, the claustrum had one of the highest densities of Y1R-ir in the rat brain comprised of a dense population of cell bodies and a varicose network of immunopositive fibers (Fig. 9D); this area is devoid of Y5R-ir (Fig. 9E). This figure illustrates the specificity of the double-label ICC where only Y1R-ir (green) is detected in the claustrum and the signal on the red (Cy3) channel is insignificant. This finding indicates that there is no bleed-through of the signal nor is there cross-reactivity of the two methods of detection.

Within the basal telencephalon, the amygdaloid complex displayed immunoreactive staining for Y1R and Y5R. Discrete populations of Y1R-immunoreactive perikarya were identified in the central and medial divisions of the extended amygdala, as well as in "cortical-like" nuclear groups of the basolateral complex (Fig. 10A,C). Y1R-ir cell bodies in the medial CeAm displayed extensive processes that were present within a rich fiber plexus (Fig. 10E). The overall intensity and presence of Y1R was stronger in the medial CeAm, which correlates well with the differential NPYergic innervation of the medial CeAm (CeM). Also prominent were populations of Y1R-immunoreactive perikarya and fibers in the lateral and medial parts of the bed nucleus of the stria terminalis (Fig. 8A,F), as well as in the medial amygdaloid (MeAm) nucleus. Y1R-immunoreactive cells in the basolateral complex were relatively homogenous populations of pyramidal-shaped cell bodies with short apical processes, interspersed among a low density of immunoreactive fibers. This pattern of immunoreactive staining extended throughout the rostral–caudal extent of the lateral and basolateral nuclei.

Immunoreactive staining for the Y5 receptor was observed almost exclusively in the basolateral amygdaloid complex with few cells observed in the lateral division of the central amygdala (Fig. 10B,D). Similar to the Y1R, Y5R-immunoreactive perikarya were homogeneously distributed throughout the lateral and basolateral complex, displaying pyramidal-shaped cell bodies with apical processes (Fig. 10F).

Diencephalon

The thalamus contained striking amounts of immunoreactive labeling for both the Y1 (Fig. 11A,C) and Y5 (Fig. 11B,D) receptors. Abundant Y1R-immunoreactive perikarya were distributed throughout most major nuclear groups, where labeled cell bodies were typically medium in size and often displayed processes with a multipolar arrangement (Fig. 11C). In contrast to the abundance of labeled cell bodies and processes, Y1R-immunopositive fibers were sparsely distributed throughout most of the thalamus with highest concentrations present in the reticular (Rt) and ventrolateral (VPL) thalamus (Fig. 11E). Y1R immunostaining extended posterolaterally into the metathalamus, and was present in the lateral (dorsal nucleus) and medial (dorsal, medial, and ventral nuclei) geniculate bodies. Dense fiber staining for the Y1R was evident in a discrete region corresponding to the junction of the medial and lateral portions of the habenula. Immunostaining for Y5R was also very abundant in the thalamus with a slightly different pattern of staining than that of the Y1R receptor. Notably, Y5R immunostaining was less in the midline nuclear groups (Table 1). Within most major divisions of the thalamus, Y5R-ir was present on multipolar cells and within fine fibers that were interspersed within nuclear groups (Table 1). Strong immunoreactive staining for the Y5 receptor was present on dispersed cells and fibers in the reticular thalamus (Fig. 11F) and displayed a high degree of colocalization with the Y1 receptor (data not shown).

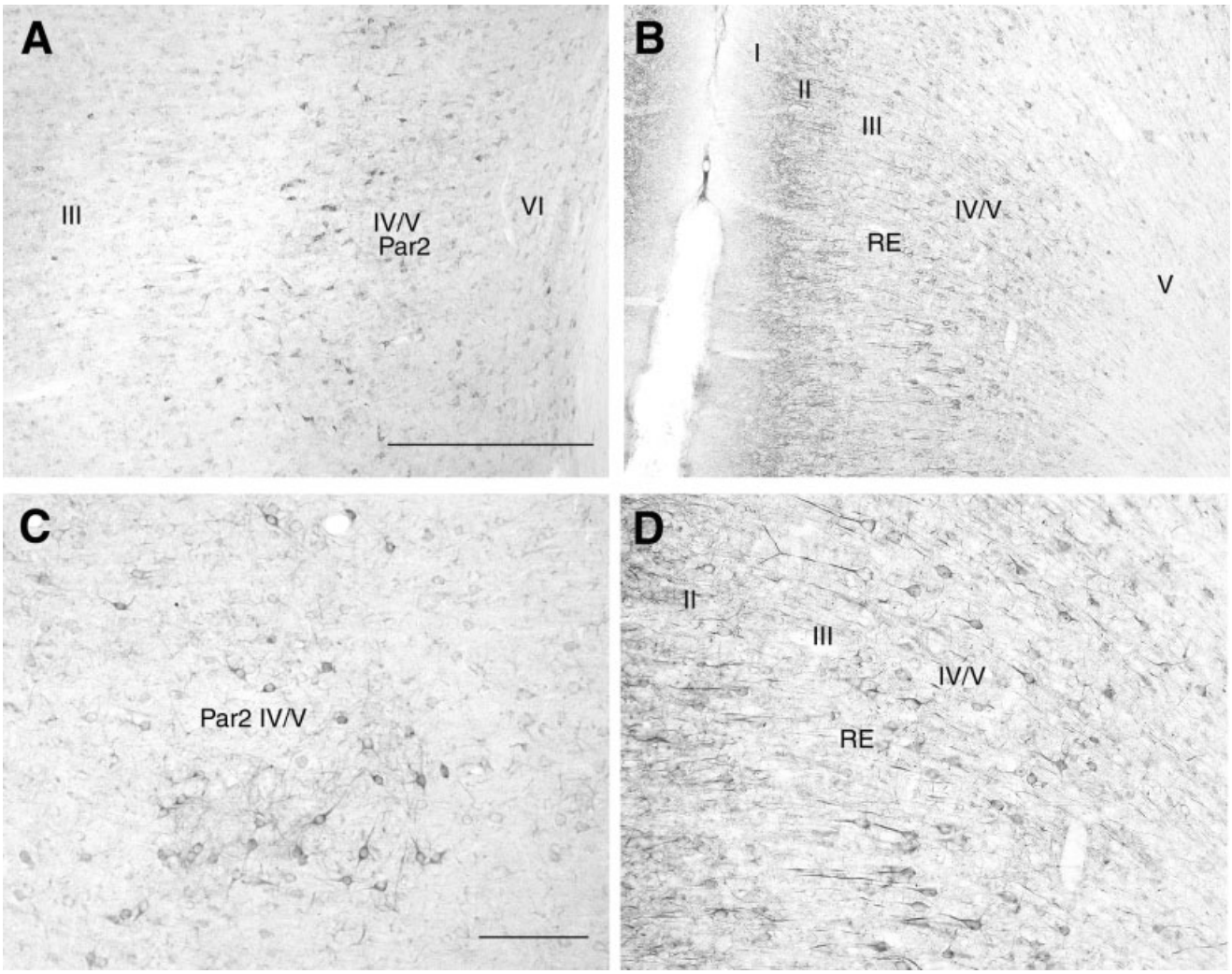

Fig. 5. Distribution of Y1 (A,C) and Y5 (B,D) immunoreactivity in the cerebral cortex. **A,C:** Y1-immunoreactive perikarya in layers IV/V in the parietal cortex. Lighter-labeled cells are evident within other cortical layers (lamina II–IV). **B,D:** Y5 receptor (Y5R) immunoreactivity in the retrosplenial cortex. Pyramidal and oval cells present within layers II and IV–V exhibit labeling as do their apical processes. For abbreviations, see list. Scale bars = 200 μm in A (applies to A,B), 100 μm in C (applies to C,D).

The hypothalamus is another region where there were notable differences in the relative concentrations and distribution of Y1R-ir and Y5R-ir (Table 1). Rostrally, the medial preoptic area (MPOA) contained a heterogeneous cell population in terms of size, morphology, and distribution, interspersed amid a diffuse network of fibers. Y1R-immunoreactive labeling extended continuously from the dorsal to the ventral aspects of the medial preoptic area, with the highest density of cell bodies and fibers observed ventromedially in regions corresponding to the medial, anteroventral, periventricular, and ventromedial nuclei. No detectable labeling was noted for the Y5 receptor in this brain region. In the suprachiasmatic nucleus (SCh), Y1R-immunoreactive perikarya and fibers were concentrated in the ventral portion of the nucleus (Fig. 12A), whereas Y5R-ir cells and fibers also extended to the dorsal aspect of the nucleus (Fig. 12B).

The hypothalamic arcuate nucleus (ArcN) contained one of the most striking clusters of Y1R-ir perikarya seen in the rat brain (Fig. 12C). These cells were located predominantly in the ventrolateral portion of the arcuate nucleus and extended laterally into the periarcuate region. A cluster of morphologically similar perikarya was also observed rostrally in the retrochiasmatic area (RCh), a brain region closely associated with the arcuate nucleus. A second population of medium, lighter labeled Y1R-immunoreactive perikarya could be distinguished within the ventromedial ArcN (ArcM) nucleus. Y1R-immunoreactive fibers were also abundant in both the medial and lateral aspects of this nucleus. In contrast to Y1R, immunoreactive staining for the Y5 receptor was concentrated on cells, not fibers, of the ArcN (Fig. 12D). Y5R-immunoreactive cell bodies were medium in size, characteristically displaying punctate immunoreactivity, devoid of processes, and were not seen in proximity to any immunopositive fibers. In some assays, it appeared that staining may be present within microglia, although further double-label studies will need to directly assess this staining. Labeling for both Y1 (Fig. 3A) and Y5

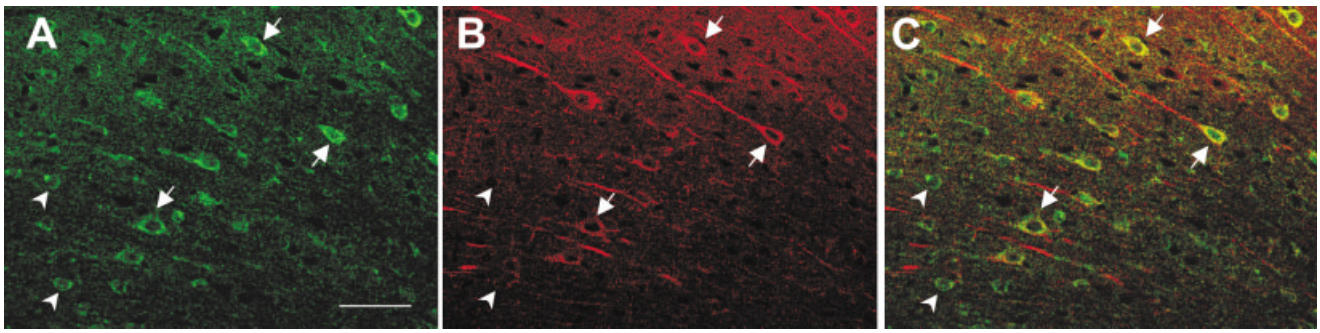

Fig. 6. Confocal images of Y1 receptor (Y1R) -immunoreactive (green; **A**) and Y5R-immunoreactive (red; **B**) cells and fibers in the retrosplenial cortex (layer IV). **C:** A merged image showing the degree of overlap between Y1R and Y5R immunoreactivities (yellow). Arrows indicate double-labeled cells, and arrowheads indicate single-labeled cells. Scale bar = 50 μm in A (applies to A–C).

(Fig. 12D) receptors was evident in the median eminence (ME).

High densities of cell bodies and processes for Y1R were observed in the anterior, dorsomedial, and ventrolateral divisions of the VMH (Fig. 3A), whereas the central division of the nucleus was relatively cell-sparse. A rich network of Y1R-immunopositive fibers was similarly distributed within the ventromedial nucleus, with the highest densities localized to cell-rich, e.g., anterior, dorsomedial, and ventrolateral nuclear divisions. Within the VMH, a relatively dense plexus of Y5R-ir, devoid of detectable cells, was present in fibers throughout the three divisions.

Abundant immunoreactive staining for Y1R was seen in the hypothalamic PVN. Y1R-immunoreactive perikarya were present in both the parvo- and magnocellular nuclear divisions (Fig. 13A,C,D). A population of small to medium cell bodies with extensive processes was seen interspersed among a high density of fibers in the parvocellular nuclear division, which could be further localized to distinct parvocellular subdivisions (Fig. 13A). A second neuronal population, having large Y1R-immunoreactive perikarya, was localized to magnocellular parts of the paraventricular nucleus. Magnocellular perikarya were characteristically devoid of processes and, with rare exception, were not observed codistributed with immunoreactive fibers (Fig. 13D). Morphologically similar populations of Y1R-immunoreactive magnocellular perikarya were also observed in the principal and retrochiasmatic portions of the supraoptic nucleus (Fig. 13E) and in accessory magnocellular nuclei (i.e., n. circularis).

Immunoreactive staining for the Y5R was present in magnocellular parts of the PVN, where medium to large cell bodies extending short processes were interspersed among a low density of fibers with punctate immunoreactivity (Fig. 13B) and within the parvocellular divisions. Of interest, the intensity of Y5R immunostaining within the magnocellular division showed a variability between animals. Whether this represents dynamic regulation of NPY Y5 receptor levels remains to be determined. As observed for the Y1R, Y5R-immunoreactive perikarya were seen in the principal and retrochiasmatic portions of the SON and in accessory magnocellular nuclei (Fig. 13F). A moderate to high density of immunoreactive fibers was observed ventral to the SON, corresponding to the glial lamina (Armstrong et al., 1982). In contrast with Y1R, few Y5R-ir cells or fibers were observed in the parvocellular PVN.

A population of Y1R-ir perikarya was observed in the dorsal hypothalamic area (Fig. 1B). Labeled cell bodies and processes were associated with a rich fiber network that displayed a similar, predominantly lateral distribution. A similar pattern of distribution was noted for the Y5R in the dorsal hypothalamus as well. Also notable at the level of the dorsal hypothalamic area were populations of Y1R-ir perikarya and fibers in the perifornical nucleus (Fig. 13A) and lateral hypothalamic area. The perifornical nucleus contained immunoreactive cell bodies concentrically arranged around the dorsal aspect of the postcommissural fornix. Y1R- and Y5R-labeled cell bodies in the lateral hypothalamic area shared a similar morphology and were observed throughout the rostrocaudal and dorsoventral extent of this brain area. These latter populations of Y1R-labeled perikarya displayed relatively few, short processes and were not seen in close proximity to any immunopositive fibers.

Mesencephalon/Metencephalon/ Myelencephalon

Immunoreactive staining for the Y1R and Y5R receptors was seen in several brainstem nuclei that are known to be principal sources of monoamine neurotransmitters in the central nervous system (CNS). Populations of small to medium, pyramidal-shaped Y1R- and Y5R-immunoreactive cell bodies were concentrated in the pars compacta of the substantia nigra (SNC) and the medially adjacent ventral tegmental area (VTA). Fibers for both receptors were observed to be localized to a narrow margin in the ventral aspect of the SNC. The SNC and VTA, collectively referred to as the "SNC–VTA complex," constitute the principal sources of dopamine in the CNS. Populations of Y1R- and Y5R-labeled cell bodies were observed in the midbrain dorsal raphé nucleus and, similarly, in the pontine median raphé nucleus, which constitute the principal sources of serotonin in the CNS (Steinbusch and Niewenhuys, 1983). One of the highest concentrations of immunoreactive staining for the Y1 and Y5 receptor was seen in the locus coeruleus (LC; Fig. 14A,B), a primary source of noradrenergic neurons in the CNS (Everitt et al., 1984; Holets et al., 1988). This dense population of small, oval to fusiform cell bodies was observed in sagittal views extending con-

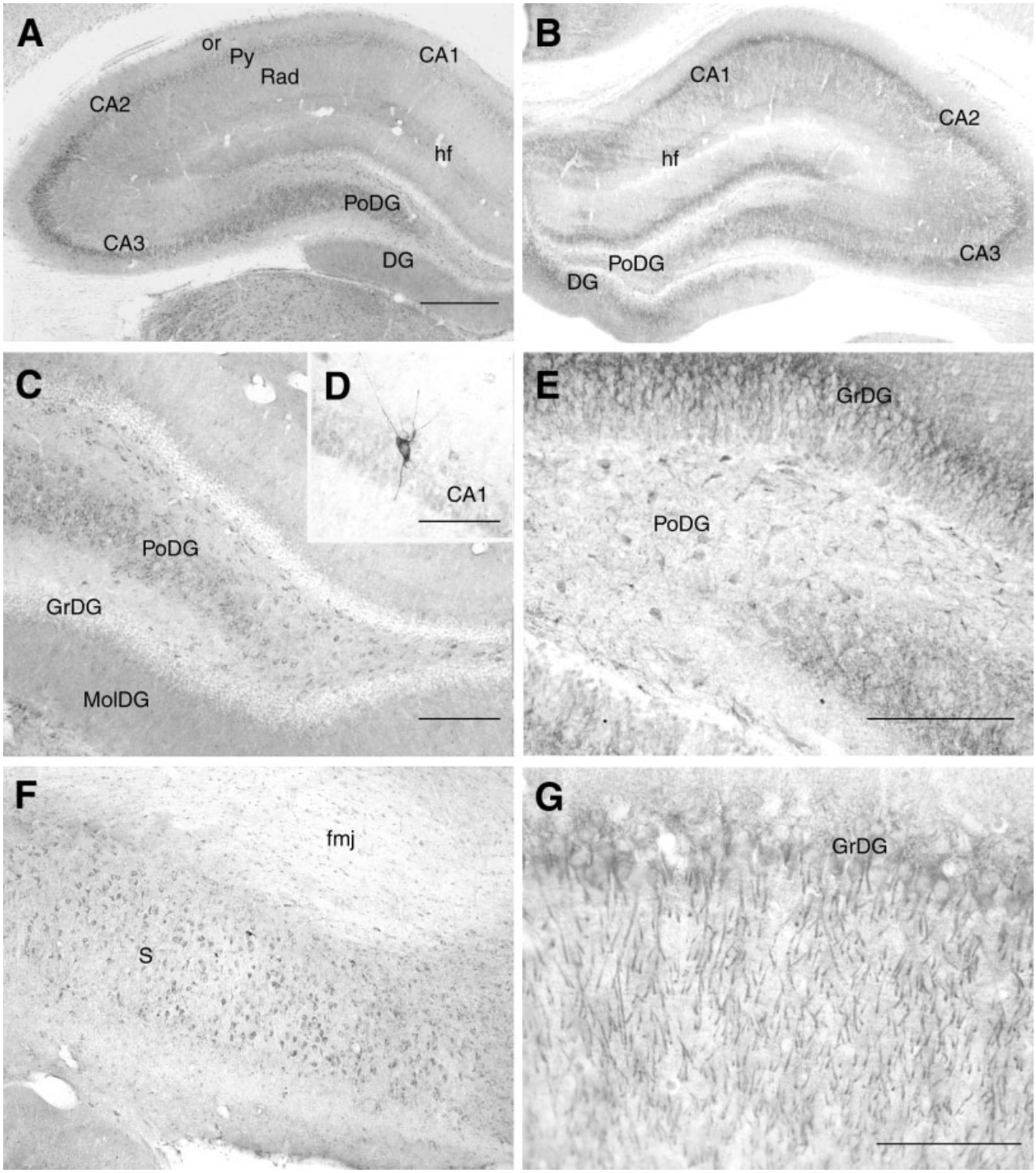

Fig. 7. Photomicrographs of Y1 receptor (Y1R; **A**) and Y5R (**B**) immunoreactivity in the hippocampus. **C:** Y1R immunoreactivity in the polymorphic and molecular layers of the dentate gyrus. Cells in the granule layer are sparsely labeled. **D:** Y1-immunopositive interneuron in the CA1 region. **E:** Demonstration of Y5R immunoreactivity on cells and process in the granule layer and within scattered cells in the polymorphic layer of the dentate gyrus. **F:** Y1R immunoreactivity on cells in the subiculum. **G:** Higher magnification of Y5R immunoreactivity on cells and fibers in the dentate gyrus. For abbreviations, see list. Scale bars = 500 μm in A (applies to A,B), 200 μm in C (applies to C,F); 50 μm in D; 200 μm in E, 100 μm in G.

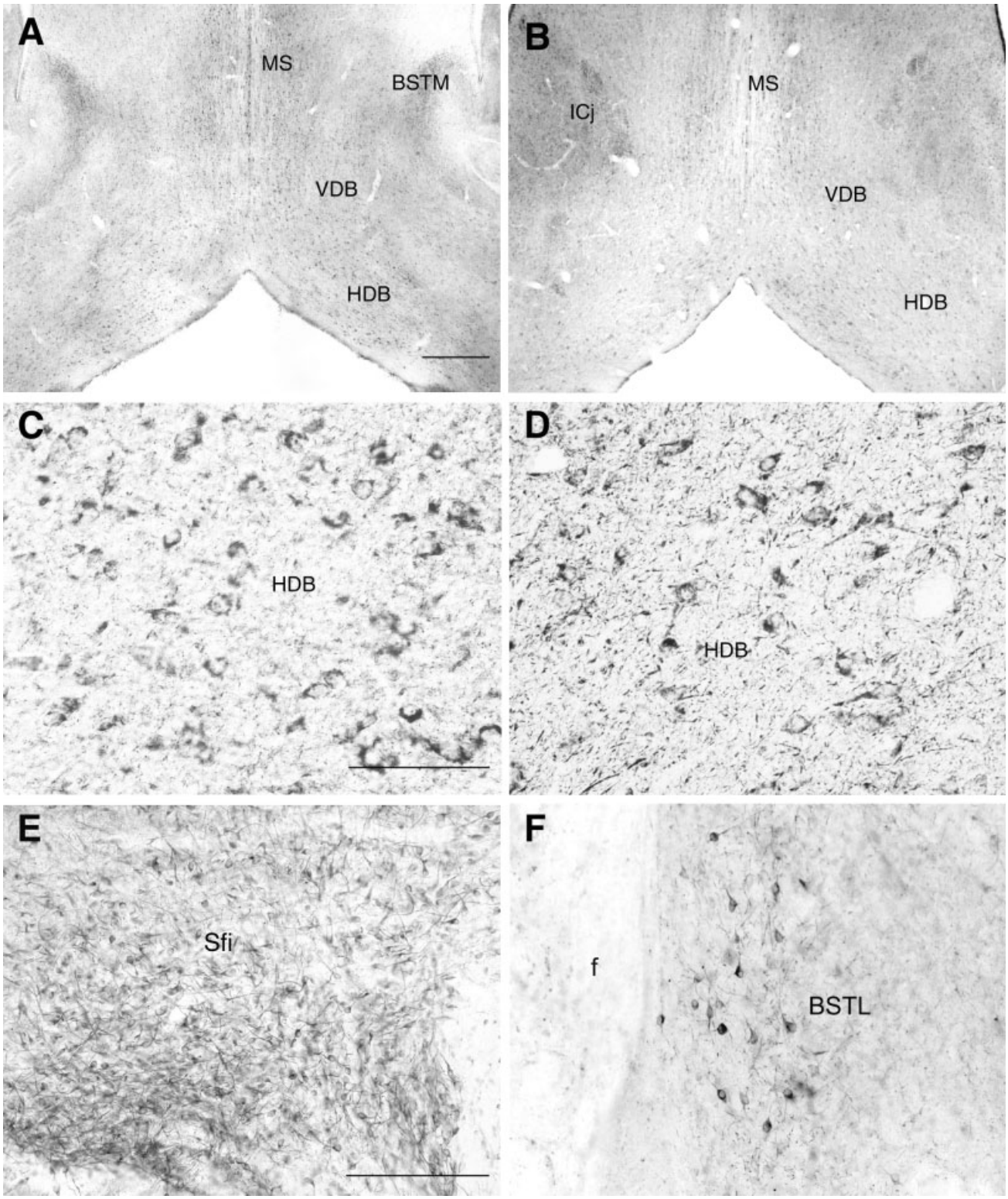

Fig. 8. Immunoreactive staining for the Y1 receptor (Y1R; **A**) and Y5R (**B**) in the medial septum-diagonal band complex. Staining for Y5R is also present in the islands of Calleja (ICj). Y1R (**C**) and Y5R (**D**) -immunoreactive cells are found dispersed in the HDB. **E:** Y1R immunostaining on cells and fibers in the Sfi. **F:** Y1R immunopositive cell and fibers are present in the lateral BNST (BSTL). For abbreviations, see list. Scale bar = 500 μm in A (applies to A,B), 100 μm in C (applies to C,D), 200 μm in E (applies to E,F).

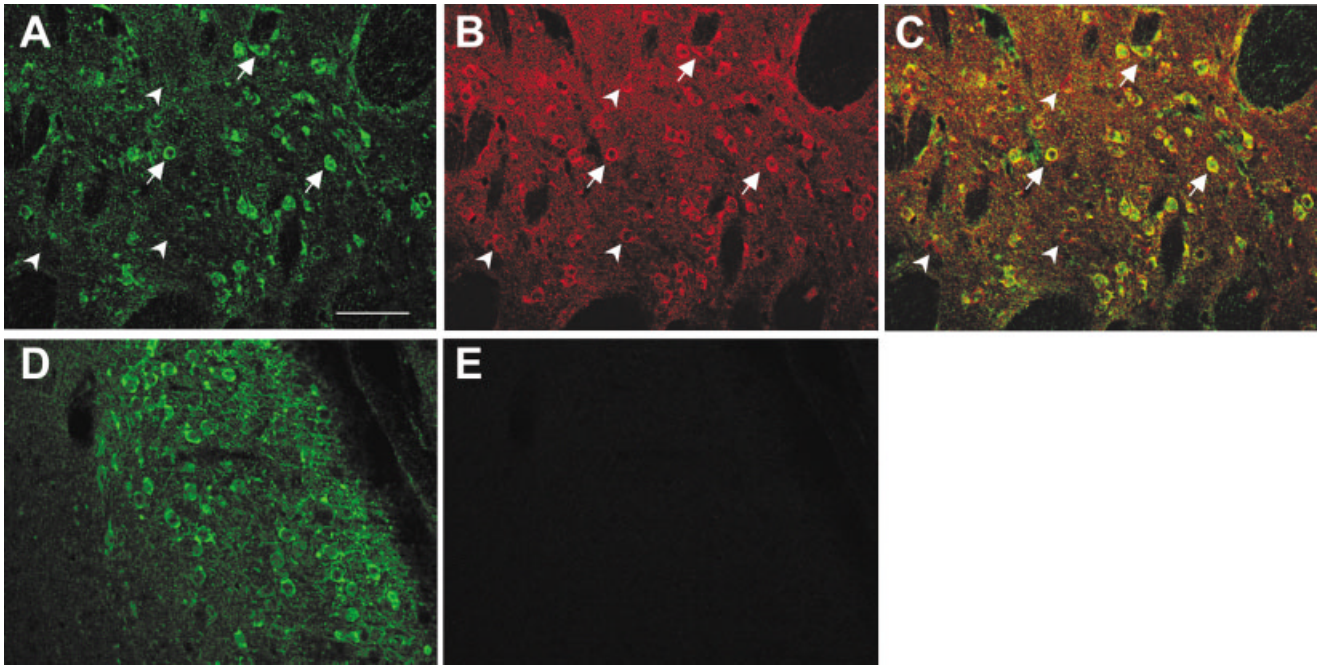

Fig. 9. Distribution of Y1 receptor (Y1R; green; **A**) and Y5R (red; **B**) immunoreactivity in cells and fibers of the caudate putamen. **C:** Colocalization (yellow) of the Y1 and Y5 receptors (indicated by arrows). Arrowheads point to cells that demonstrate a single label. **D:** Y1R immunoreactivity in the claustrum. **E:** Absence of Y5R immunoreactivity in the claustrum. Scale bar = 50 μm in A (applies to A–E).

tinuously along the rostral–caudal extent of the nucleus, and into the ventrally adjacent subcoeruleus. All of the aforementioned populations of Y1R-ir perikarya displayed short to moderate processes and were not observed in close proximity to any immunopositive fibers. Similar to the Y1 receptor, Y5R-labeled perikarya extended continuously along the rostral–caudal extent of the locus coeruleus and into the subcoeruleus. In contrast, Y5R-ir cell bodies displayed relatively long processes and were embedded in a dense network of immunopositive fibers (Figs. 1C, 14B).

Populations of Y1R- and Y5R-ir perikarya were localized to several cranial nerve nuclei. The trigeminal system, including both sensory and motor components, displayed a particularly rich immunoreactive staining for both NPY receptors (Fig. 14A,B). The motor trigeminal nucleus (Mo5) contained a population of large Y1R-immunoreactive, fusiform cell bodies with short processes of a predominantly bipolar arrangement. A similarly large-sized population of Y1R-immunoreactive perikarya was seen in the mesencephalic (sensory) trigeminal nucleus (Me5, Fig. 14A). In contrast to Mo5, this neuronal population displayed predominantly oval cell bodies with no apparent processes. Neither of the latter populations of Y1R-immunoreactive perikarya were seen in association with immunopositive fibers. Small to medium Y1R-labeled cell bodies with long processes were also observed concentrated in the dorsal pole of the spinal nucleus of the trigeminal nerve. This population of neurons was embedded in a rich network of labeled fibers that coursed dorsoventrally throughout the superficial lamina of the spinal trigeminal nucleus.

Y1R- and Y5R-immunoreactive perikarya were also localized to the oculomotor (medial accessory), hypoglossal, and vagal (dorsal motor) nuclei (Fig. 14A–D). Labeled neurons in the respective cranial nerve nuclei were morphologically similar, displaying medium to large, oval cell bodies without processes and were not seen in proximity to immunopositive fibers. A similar staining pattern was observed for the Y5 receptor. A low density of Y1R-immunoreactive perikarya was observed in the interstitial subnucleus of the nucleus tractus solitarius (nts), a major termination site for vagal (superior laryngeal branch) sensory afferents (Kalia and Fuxe, 1985). This neuronal population exhibited small, fusiform-shaped cell bodies with long processes having a bipolar arrangement and were embedded in a high density of varicose fibers (Fig. 14C).

Immunoreactive staining for both Y1 and Y5 receptors was observed in several brainstem nuclei involved in cerebellar functioning, e.g., precerebellar nuclei (Ruigrok and Cella, 1995), including the retrotegmental pontine nucleus, lateral reticular nucleus (magnocellular part), and inferior olive nuclear complex. Y1R-immunoreactive neurons in these precerebellar nuclei displayed oval to pyramidal cell bodies, typically without processes, and were not seen in association with labeled fibers. A similar immunoreactive staining pattern was associated with Y1R-labeled perikarya in the magnocellular part of the red nucleus, also known to have an important role in cerebellar functioning. Within the cerebellum, a population of large, oval Y1R- and Y5R-immunoreactive cell bodies were seen in the Purkinje cell layer (Fig. 14A,B). Strong fiber staining for the Y5 receptor was seen on processes of the Purkinje cells. The presence of binding sites in this region has been documented, although there appears to be little NPY innervation to the cerebellum.

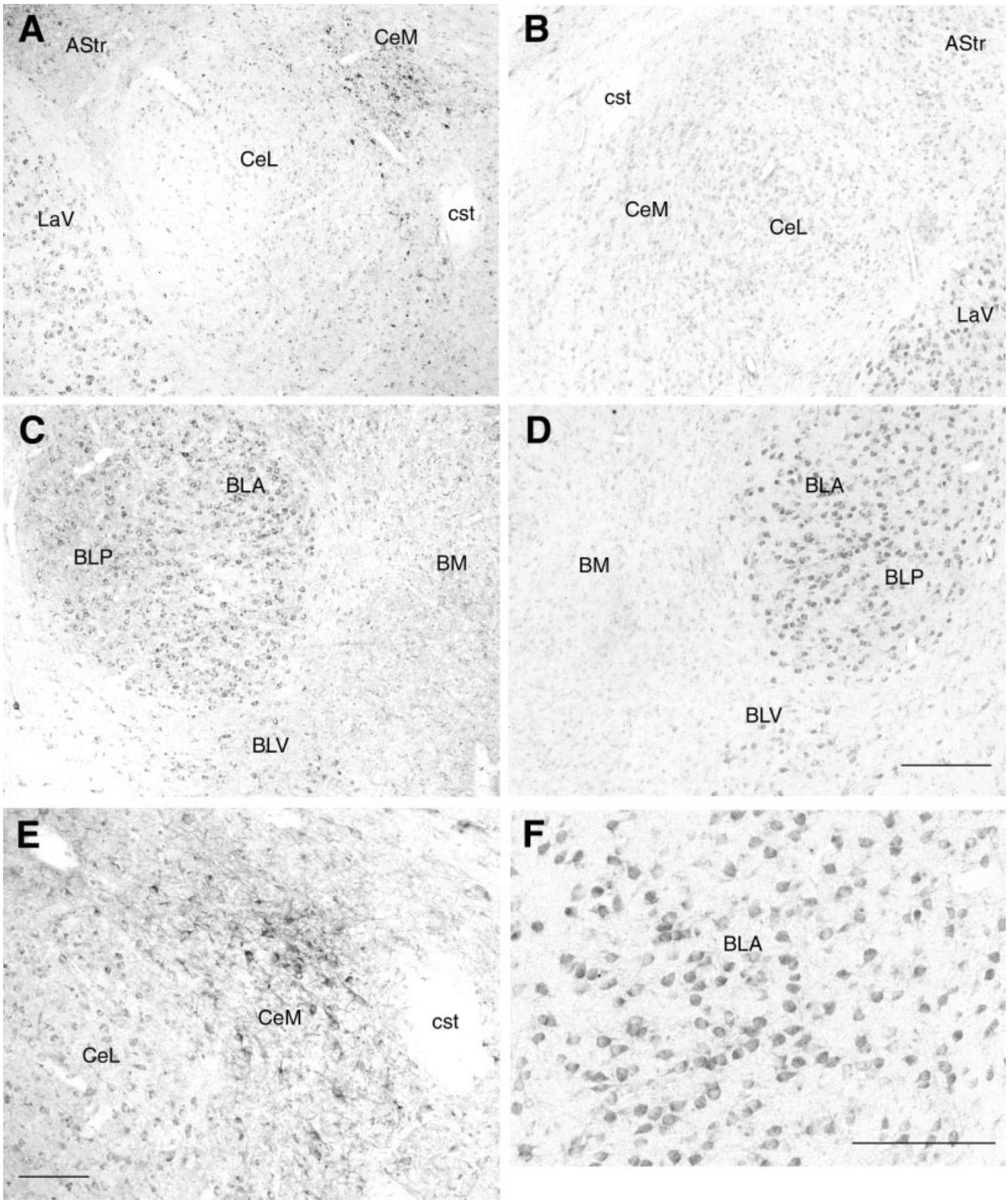

Fig. 10. Photomicrographs of Y1 receptor (Y1R; **A,C**) and Y5R (**B,D**) immunoreactivity in the amygdaloid complex. Y1R (bregma -2.56 mm) and Y5R (bregma -2.80 mm) immunoreactivity is present on cells in the lateral and basolateral divisions of the amygdala. **E:** Y1R expression on cells and fibers within the lateral (CeL) and medial (CeM) division of the central amygdala. **F:** Higher magnification of Y5R-expressing cells in the BLA. For abbreviations, see list. Scale bar = 200 μm in D (applies to A–D), 100 μm in E, 200 μm in F.

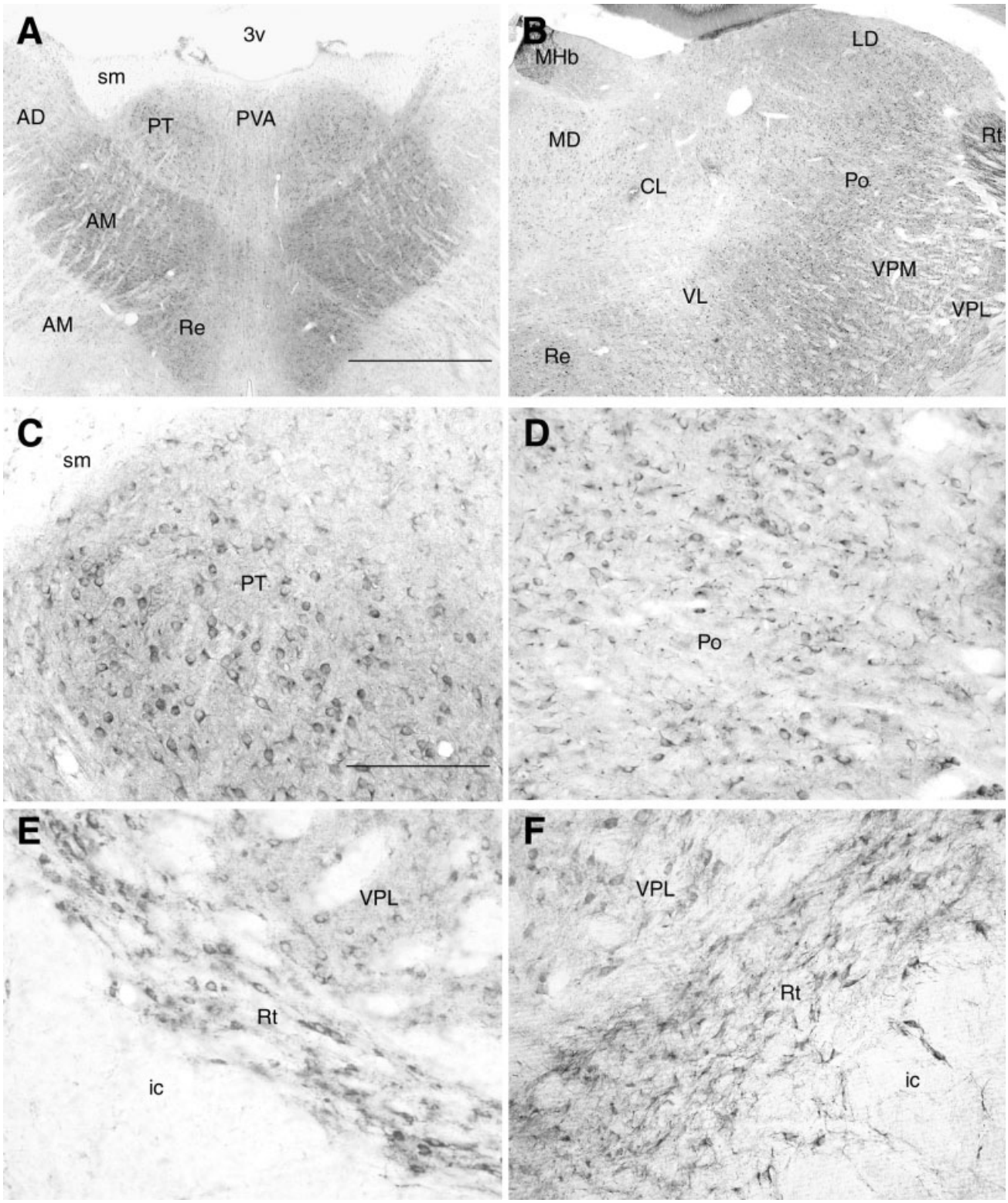

Fig. 11. Y1 receptor (Y1R; **A**; bregma -1.40 mm) and Y5R (**B**; bregma -2.80 mm) immunoreactivity in the thalamus. **C:** Higher power magnification of Y1R-immunopositive cells in the parataenial n. (PT), showing medium cells with a predominantly bipolar arrangement. **D:** Y5R-immunopositive cells in the posterior thalamus (Po). Y1R (**E**) and Y5R (**F**) -immunoreactive cells and fibers are prominent in the reticular and ventroposterolateral (VPL) thalamic nuclei. For abbreviations, see list. Scale bars = 500 μm in A (applies to A,B), 200 μm in C (applies to C–F).

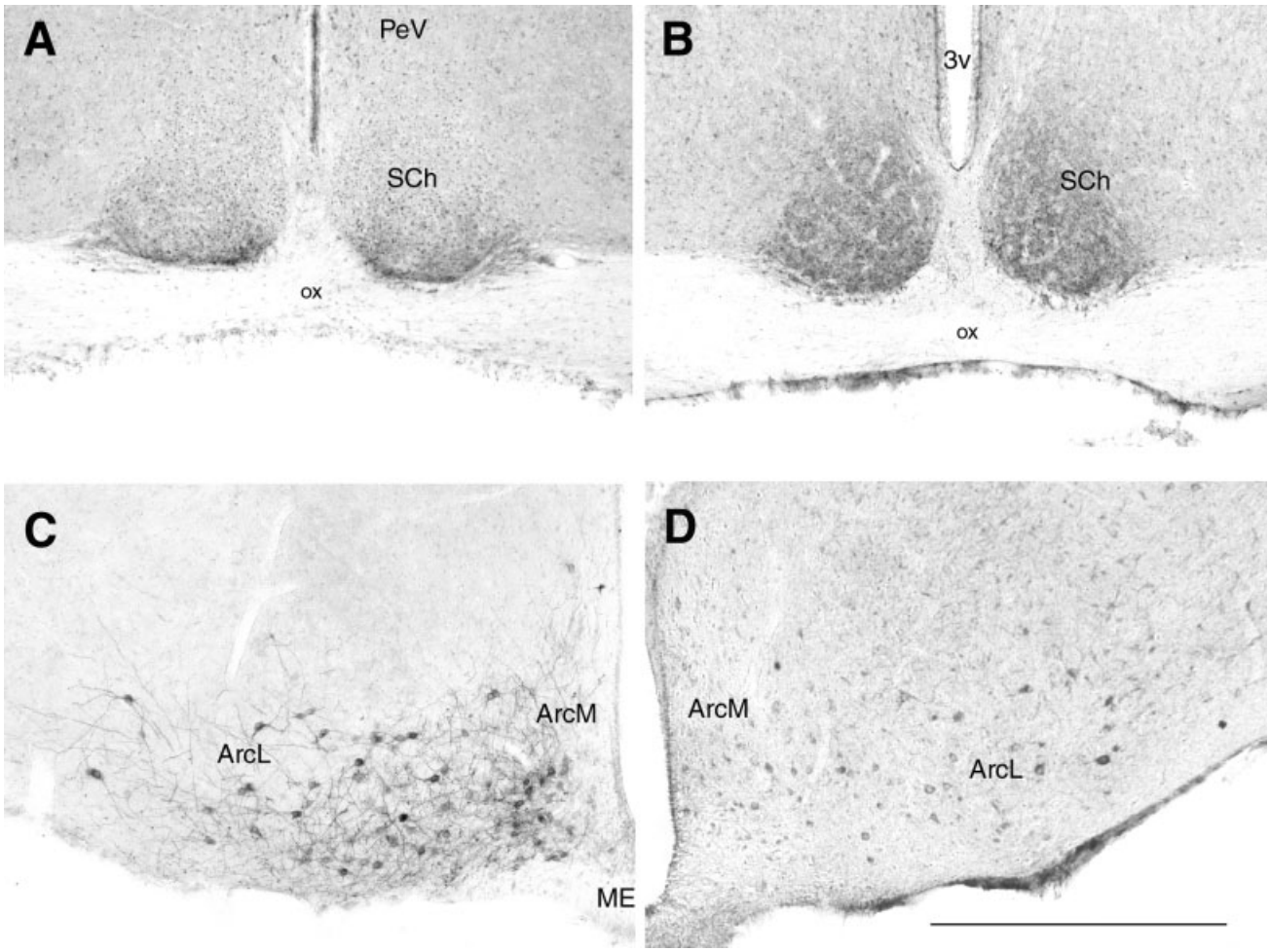

Fig. 12. Immunoreactive staining for Y1 receptor (Y1R; **A**) and Y5R (**B**) cells and fibers in the SCh, primarily distributed in the ventral portion of the nucleus. **C:** Y1R-immunoreactivity in the ArcN. Tissues were treated with 0.1% Triton to increase the visibility of the extensive fiber distribution of Y1R. **D:** Y5R immunoreactivity on cells within the ArcN and fibers in the median eminence (ME). For abbreviations, see list. Scale bar = 500 μm in D (applies to A–D).

DISCUSSION

The present study is a comprehensive comparison of NPY Y1 and Y5 receptor immunoreactivities in the male rat brain by using newly developed polyclonal antisera. The antibodies were generated against the last 20 amino acids (363-382) of the rat Y1R protein and 20 amino acids of an internal sequence corresponding to extracellular loop 3 (400-420) of the Y5R protein. The widespread distribution of Y1R-ir was quite striking, being present in cell bodies and fibers throughout the rostral–caudal extent of the brain. The Y5R was also fairly widely distributed, although not to the same extent as Y1R (Table 1). The specificity of these antibodies was assessed by using preimmune serum and peptide preadsorption controls, which prevented detectable signals in immunocytochemical assays and Western analysis blots. Antibodies generated against different regions of these receptor proteins demonstrate similar patterns of immunostaining (Zhang et al., 1994; Caberlotto et al., 1998; Kopp et al., 2002). Overall, our findings are consistent with the presence of Y1 and Y5 receptor mRNA and protein levels as assessed by using immunocytochemistry (Grove et al., 2000; Migita et al., 2001; Campbell et al., 2001; Kopp et al., 2002), in situ hybridization (Mikkelsen and Larsen, 1992; Parker and Herzog, 1999; Durkin et al., 2000), receptor autoradiography (Quirion et al., 1990; Dumont et al., 1998b), electrophysiology (Sun et al., 2001; Pronchuk et al., 2002), and pharmacologic studies (Kask et al., 1998b; Sajdyk et al., 1999; Niimi et al., 2001). With few exceptions, Y1 and/or Y5 receptor-ir shows a strong correlation with the known distribution of NPY-immunoreactive terminals (Allen et al., 1983; de Quidt and Emson, 1986).

The mapping studies presented describe the extent of Y1 and Y5 receptor-ir using a standard double-antibody staining protocol with the signal being visualized with a DAB (diaminobenzidine)-Ni+ intensification. By using this method, we are able to visualize considerable cell body and fiber staining within regions that are known to be responsive to NPY and observe signals that are comparable to those previously described (Zhang et al., 1994; Grove et al., 2000; Campbell et al., 2001). In comparison with the recent study by Kopp et al. (2002), we observe

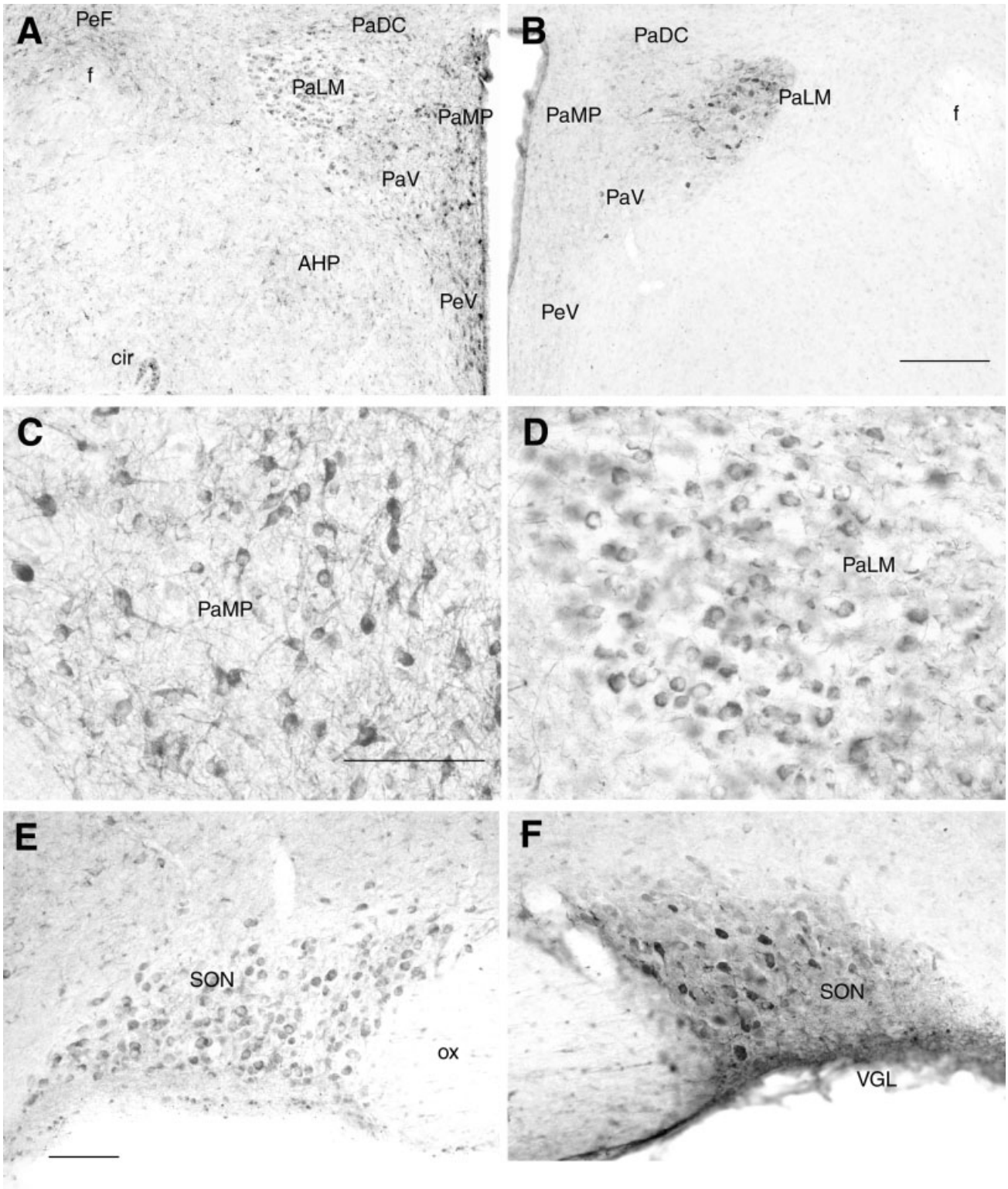

Fig. 13. Y1 receptor (Y1R; A) and Y5R (B) immunostaining in the hypothalamic PVN and SON. **A:** Y1R immunoreactivity is also present on fibers and cells in the PeF and periventricular n (PeV) and the n. circularis (cir). **B:** Light Y5R immunostaining can be seen on cells extending into the PeV. Y5R is strongest in the magnocellular division with lighter staining on cells and a few fibers in the parvocellular PVN. Higher magnification of Y1R immunoreactivity in the parvocellular (**C**) and magnocellular (**D**) PVN. Y1R (**E**) and Y5R (**F**) -immunopositive cells in the SON. Y5R immunoreactivity is also present on fibers of the ventral glial lamina (VGL). For abbreviations, see list. Scale bars = 200 μm in B (applies to A,B), 100 μm in C (applies to C,D), in E (applies to E,F).

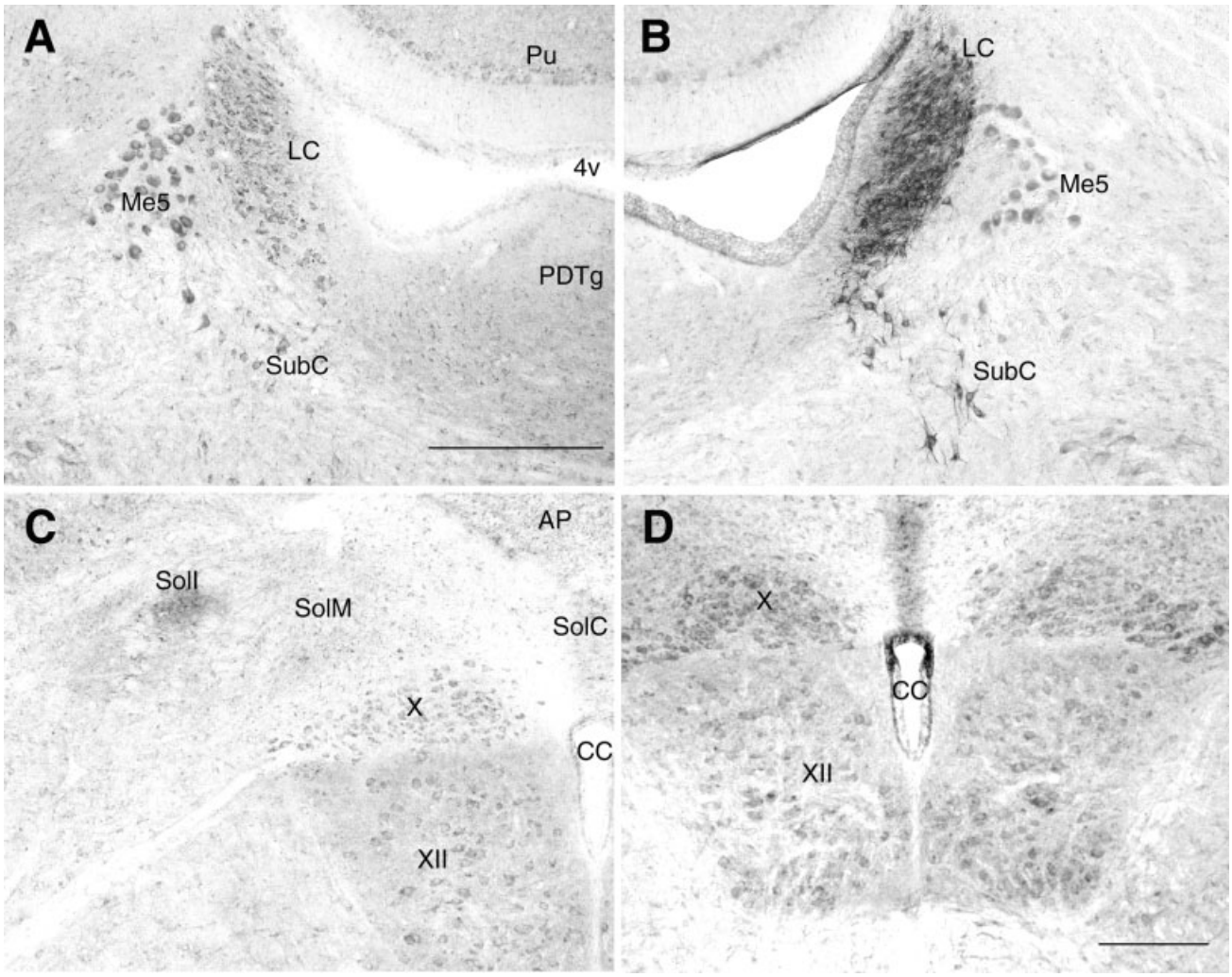

Fig. 14. Coronal sections showing Y1 receptor (Y1R; **A**) and Y5R (**B**) immunoreactivity in the locus coeruleus (LC) and subcoeruleus (subC). The Me5 and cerebellar Purkinje cells and fibers demonstrate labeling for both receptors. Comparative distribution of Y1R (**C**) and Y5R (**D**) immunoreactivity in the caudal medulla. Both receptors are present on cells within the SolM, X, and XII. For abbreviations, see list. Scale bars = 500 μm in A (applies to A,B), in D (applies to C,D).

more Y1R-positive cell bodies in several regions (e.g., thalamus, magnocellular paraventricular hypothalamus, and basolateral amygdala). As our antibodies are directed to similar regions of the Y1R protein, the few differences between our results may be attributable to the use of different detection methods or the use of Triton in the immunostaining protocol. In initial studies, the use of Triton at concentrations as low as 0.1%, decreased the detection of Y1R in cell bodies in certain regions, such as the thalamus, magnocellular PVN, and amygdala. It may be that the detergent-like actions of Triton disrupts membrane-associated Y1R protein perhaps either by removing it from the membrane or altering its epitope and, hence, its detection by the antibody. This effect of Triton on receptor immunoreactivity has been demonstrated in other systems (Decavel and Curras, 1997). There was a similar, yet less striking, effect of Triton on Y5R-immunoreactive staining.

Both antibodies show characteristic staining on cell membranes as well as in cell bodies, fibers, and cytoplasm. This distribution of Y1R immunostaining in these compartments is supported by Western analysis of hypothalamic tissue where immunoreactive bands are present in both the membrane- and cytosol-enriched fractions. By using Western analysis, two bands were observed for the Y1R in the membrane-enriched protein preparations from hypothalamic tissue: a low (~42 kDa) and a high (85–90 kDa) molecular weight band for Y1R. The cytosol-enriched fraction from hypothalamus demonstrated only the higher molecular weight band. The presence of the ~42-kDa band in the membrane-enriched fraction likely represents a monomeric form of the membrane-bound receptor, whereas the higher molecular weight band could represent a dimerized form of the receptor. The presence of multiple bands for the Y1R has been reported previously (Migita et al., 2001) and suggested to be a product of posttranslational processing or glycosylation. There are several N-linked glycosylation sites in the N-terminus for the Y1 receptor, which may account for the different molecular weight bands. It is equally likely that this higher

molecular weight protein could reflect synthesis of a pro-receptor protein before insertion into the membrane. The presence of a 85- to 90-kD molecular weight band in the cytosol-enriched fraction is more open to interpretation. As this is a relatively crude preparation, there may be some membrane proteins in this fraction or the receptor could be bound to other cytosolic compounds, such as G proteins. Western analysis showed a double band for the Y5 receptor in hypothalamic tissue and no Y5-immunoreactive bands were detected in Western blots of SK-N-MC homogenates, which convincingly demonstrated that the Y5R antiserum does not cross-react with the Y1 receptor.

Overall, we observe good correlation between the presence of Y1 and Y5 receptor protein in regions that are rich with NPYergic fibers (Allen et al., 1983; de Quidt and Emson, 1986). There are a few regions where receptor protein is detected without strong NPY immunostaining. The islands of Calleja contain few NPY fibers, whereas both Y1 and Y5 receptor-ir were prevalent. Additionally, the thalamus, which contains striking immunostaining for both receptor subtypes, is not endowed with many NPY fibers. However, application of NPY to thalamic neurons elicits changes in neuronal firing, indicating that functional receptors are present (Sun et al., 2001). In the midbrain and brainstem regions, Y1R and Y5R are also seen in the geniculate (DLG), medial mammillary nucleus, superior colliculus, vestibular nuclei, and spinal trigeminal nuclei. These regions contain few NPYergic fibers. The cerebellum contains Y1R- and Y5R-ir on Purkinje cells and fibers, which has been noted by others (Parker and Herzog, 1999; Kopp et al., 2002). NPY receptors are also found within components of the olivary complex (LSO), which also do not receive strong NPY innervation. These mismatches of ligand and receptor have been discussed in the literature, and it is possible that NPY reaches these receptors by volume transmission (Fuxe et al., 1991) or that there are additional members of the NPY ligand family that have yet to be identified (Herzog et al., 1995).

Whereas the Y1 and Y5 receptors have long been presumed to be postsynaptic receptors, with the Y2R being the primary presynaptic receptor, several histochemical and physiological studies indicate that Y1R and Y5R may also have presynaptic actions. The data presented here and in other studies demonstrate the presence of Y1R- and Y5R-ir on fibers (Campbell et al., 2001; Kopp et al., 2002; Glass et al., 2002), suggesting that activation of these receptors could modulate presynaptic neurotransmitter release. Studies using electron microscopy have shown that Y1R-ir is present within nerve terminal regions that also contain NPY, thereby providing anatomic evidence for a presynaptic role for NPY, perhaps in regulating its own release (Pickel et al., 1998; Glass et al., 2002). The distribution of the Y5R has not yet been examined by using ultrastructural analysis.

A major point addressed by this work is the comparison of the distribution of Y1R-ir and Y5R-ir in the rat brain. There is considerable overlap in the distribution of Y1R-ir and Y5R-ir with the Y1R being more widely dispersed and present to a larger degree on fibers. Parker and Herzog (1999) presented a mapping of Y1R and Y5R mRNA by using in situ hybridization and demonstrated that the expression of Y1R and Y5R was distributed throughout the brain, with Y5R mRNA expression always coinciding with that of Y1R mRNA. The issue that has not yet been addressed is whether these two receptors are colocalized. The Y1R and Y5R genes, unlike the other NPY receptor subtypes, are in close proximity to each other and have likely evolved from a gene duplication event (Herzog et al., 1997). More interestingly, there is overlap between the sequence of the Y1R (exon 1C) and the Y5R (third intracellular loop), which includes the internal intron sequence from the Y1R, in opposite orientation, in the promoter region of the Y5R gene. It has been suggested that this novel overlapping sequence may result in the coordinated expression of Y1 and Y5 receptors within the same cell. Whether this results in one or the other receptor being solely expressed or coordinately regulated in the same cell is not known. Whereas in situ hybridization ascertains the biosynthetic activity of the cell with high sensitivity, immunocytochemistry has the added advantage of being able to visualize the distribution of the actual protein within cells and fibers of given cells, which not only refines the distribution of these receptors but also adds to possible mechanisms of action (i.e., pre- vs. postsynaptic) for NPY in these regions. A specific double-label immunofluorescence protocol has been used to begin to address the coexpression of Y1 and Y5 receptors in the same cell. Within the scope of this report, Y1 and Y5 receptor colocalization has been demonstrated in cells of the cerebral cortex (predominantly in layer IV/V) and the caudate putamen. Additional analysis indicates that these receptors are also colocalized in the CA1–3 regions of the hippocampus and the reticular thalamus. Of interest, there are regional differences in the relative number of cells that coexpress the two receptors: in the cerebral cortex, nearly all Y5R-immunoreactive cells coexpress the Y1R while there are populations of single-labeled Y1R-immunoreactive cells; in the caudate putamen, populations of Y5R- and not Y1R-immunoreactive cells exhibit single label. These data are important in that they demonstrate colocalization of Y1 and Y5 receptor-ir in the same cell and that different brain regions exhibit varying degrees of colocalization. This is an important finding as the difference in the degree of colocalization may reflect an overall difference in Y1 versus Y5 receptor tone in a given area.

Within the telencephalon, immunostaining was observed for both the Y1 and Y5 receptors within the cerebral cortex, hippocampal formation, and amygdala complex. In the cerebral cortex, immunoreactive fibers for both Y1 and Y5 receptors were observed traversing through the different cortical layers (I–VI), although the overall staining pattern for Y5R was stronger and more prevalent in the cingulate/retrosplenial and piriform cortices. Similar patterns of distribution for these receptors within these regions have been noted using other antibodies (Caberlotto et al., 1998; Grove et al., 2000; Migita et al., 2001), binding, and in situ hybridization studies (Gehlert and Gackenheimer, 1997; Dumont et al., 1998b; Naveilhan et al., 1998; Parker and Herzog, 1999). That the Y1 and Y5 receptors overlap in this region has been supported by double-label immunofluorescence showing colocalization of these receptors within the same cells in the cingulate cortex (Fig. 6) as well as somatosensory cortex (data not shown). Within the cingulate cortex, some of the Y5-positive cells are colocalized with GABA and choline acetyl transferase (Caberlotto et al., 1998; Grove et al., 2000), providing a downstream circuit whereby NPY can influence the activity of cortical neurons.

Both Y1 and Y5 receptors are present within the hippocampal formation where they play an important role in modulating neural excitability and seizure thresholds (Marsh et al., 1999; Ho et al., 2000; Guo et al., 2002). The overall distribution of Y1R and Y5R in the hippocampus is similar, although there are differences in the distribution of the proteins. Y1R immunostaining is stronger on the CA2–3 regions with intense immunostaining occurring on interneurons within CA1–3. In the dentate gyrus, the majority of immunostaining for the Y1R is present on cells within the polymorphic layer, with no detectable staining on cells in the granule layer yet there is considerable Y1R fiber staining in MolDG, which has also been observed in other studies (Kopp et al., 2002). The Y5R antibody lightly labeled cell bodies within CA1–3 while staining proximal dendrites that extend into the stratum radiatum; this labeling pattern was also observed in the dentate gyrus, where cells in the granule layer also expressed Y5R. Current studies indicate that, at least within subpopulations of cells in the stratum pyramidale, there is coexpression of both Y1R and Y5R, suggesting that both of these receptors contribute to the functioning of these cells. Additional studies identified that a large portion of Y5-immunoreactive cells in the hilar region of the hippocampus contained GABA-ir (Grove et al., 2000). Preliminary studies in our laboratory indicate that a large proportion of Y1R-immunopositive interneurons in the CA1–3 region are GABAergic (Teppen and Urban, unpublished observations). These studies suggest that NPY, acting through the Y1 and Y5 receptors, may influence hippocampal activity through modulation of GABA neurotransmission.

Another prominent role for Y1 and Y5 receptors is in the amygdala, where NPY has anxiolytic actions (Wahlestedt et al., 1993; Heilig et al., 1993; Sajdyk et al., 1999; Kask et al., 2002). The presence of NPY receptors in this region is also important with respect to the generation of autonomic and behavioral responses to stress and anxiety (Gray et al., 1989; Gray, 1991). Y5R immunostaining is primarily restricted to the BLA, whereas that of the Y1 receptor is more widely distributed, extending to the CeAm and MeAm. Recently, it has been demonstrated that the anxiolytic actions of NPY are specific to the BLA through activation of Y1 and Y5 receptors (Sajdyk et al., 1999, 2002). Whereas the actions of NPY on Y1 and Y5 receptors has been demonstrated pharmacologically, there is little, if any, significant expression of receptor protein in these areas by autoradiography (Ohkubo et al., 1990; Dumont et al., 1993). The current demonstration of Y1R- and Y5R-ir in the BLA supports these pharmacologic findings and provides more information as to how NPY might alter anxiety-related behaviors. Given the low incidence of NPY receptor immunostaining on fibers in the BLA, it is likely that activation of Y1 and Y5 receptors influences the activity of cells postsynaptically. As the morphology of these cells is similar, it would not be surprising to find colocalization of Y1R and Y5R. Additional studies are needed to further examine the neurotransmitter content and projections of these Y1R- and Y5R-immunoreactive cells as they relate to the role of NPY in modulating anxiety and related behaviors. These future studies are potentially important, as some clinical treatments of anxiety have significant actions in the amygdala (Pesold and Treit, 1995; Sajdyk and Shekhar, 1997) and may influence or modulate the activity of NPY and its receptors in this region (Ehlers et al., 1997). The distribution of Y1R-ir in the CeAm closely reflects the staining for NPY, in that more Y1R-ir is found in the medial division of the CeAm (fibers and cells) with less immunostaining in the lateral aspect of this nucleus. NPY in this region may participate in the anxiolytic actions of the peptide (Heilig et al., 1993) or it may influence hormonal and cardiovascular rather than behavioral responses to a stressor (Gray et al., 1989; Gray and Bingaman, 1996; Roozendaal et al., 1997).

Immunoreactivity for both the Y1 and Y5 receptors is present throughout the hypothalamus and anatomically defines sites of action for these subtypes in regulating hormone secretion (Wahlestedt et al., 1987; Pelletier et al., 1994; Urban et al., 1996), feeding (Stanley et al., 1985, 1993), and circadian rhythms (Biello, 1995). Y1R-ir in the diagonal band of Broca (DBB) and median eminence corresponds with the roles of NPY and the Y1R in stimulating the production (Pelletier et al., 1994) and release of gonadotropin-releasing hormone (GnRH) from the hypothalamus (Kalra et al., 1992; Besecke and Levine, 1994; Besecke et al., 1994; Urban et al., 1996). Recently, it has been postulated that activation of Y5R contributes to the inhibitory actions of NPY on reproductive hormone secretion (Raposinho et al., 1999). Y5R-ir is present in the DBB and preoptic hypothalamus and has been shown to be colocalized in GnRH cell bodies (Campbell et al., 2001).

Within the PVN, intense immunostaining for Y1R was present on parvo- and magnocellular neurons as well as on numerous fibers within the parvocellular division. This finding is different than previous reports, indicating the lack of Y1R-ir in the magnocellular PVN of the mouse (Broberger et al., 1999). These discrepant results could be the result of species differences or the use of colchicine in the previous study. Y5R-ir is displayed on cells in the magnocellular PVN and on scattered cells and fibers within the parvocellular division. At least within the magnocellular PVN and SON, it is conceivable that these receptors are colocalized within the same cell. The presence of Y1R- and Y5R-ir on magnocellular PVN and SON suggests that activation of these receptors may influence the synthesis and/or release of oxytocin (OT) and vasopressin (VP). Both in vivo and in vitro studies demonstrate that NPY dose dependently stimulates vasopressin (Leibowitz et al., 1988; Liu et al., 1994; Larsen et al., 1994) and oxytocin synthesis and secretion (Kapoor and Sladek, 2001). Administration of NPY and the Y1 and Y5 receptor preferring ligand [Leu^{31}Pro^{34}]NPY excites vasopressin cells, stimulates release in vitro (Khanna et al., 1993; Kapoor and Sladek, 2001), and enhances both VP and OT release by phenylephrine, an α_1 receptor agonist. That NPY actively participates in the osmotic regulation of hormone secretion is suggested by the increase in NPY mRNA and protein levels observed in the PVN and SON after chronic osmotic stimulation (Larsen et al., 1993). The presence of Y1R- and Y5R-ir in the parvocellular division further supports a role for these receptors in the regulation of corticotropin releasing hormone (Hastings et al., 2001) and thyrotrophin releasing hormone secretion (Michalkiewicz and Suzuki, 1994). As both Y1 and Y5 receptor-ir is present within cell bodies of the PVN and median eminence, it is likely that activation of either or both of these receptors directly influences the synthesis and release of hypothalamic releasing factors.

One major, and clinically relevant, effect of NPY is its role in the induction of feeding at a number of sites,

including the PVN, lateral, dorsomedial, and perifornical hypothalamic areas (Stanley et al., 1985, 1993). The NPY receptor subtype mediating these actions has been open to debate, although there is overwhelming evidence to support a role for both the Y1 and Y5 receptors in this process. The distribution of Y1R- and Y5R-ir provides evidence that both receptors are present within these "feeding areas" of the hypothalamus. That these receptors in the PVN participate in feeding has been documented (Stanley et al., 1986; Gerald et al., 1996; Kask et al., 1998b; Yokosuka et al., 1999), although the actual mechanism underlying these actions of NPY has not been elucidated. The presence of both Y1R and Y5R protein in this region indicates that both may participate in the production of feeding responses. The regulation of these receptors under different conditions is important. Food restriction increases the expression of Y1R mRNA (Xu et al., 1998a) and alternately decreases Y5R expression (Widdowson, 1997). This finding may reflect coordinate regulation of the Y1 and Y5 receptors as discussed by Herzog et al. (1997). The perifornical area and LHA contain a striking density of Y1-immunoreactive fibers and scattered Y1- and Y5-immunoreactive cell bodies and fibers. This region of the brain receives inputs from the hypothalamic arcuate NPYergic pathway and contains a population of melanin-concentrating hormone (MCH)- and orexin-containing cells (Elias et al., 1998), which are devoid of Y1R-ir (Campbell et al., 2003). Whether the NPY receptors are present on MCH-containing cells is not known. In addition to these hypothalamic sites of action for NPY, there are additional, nonhypothalamic, sites that are also important in initiating feeding behavior (Broberger and Hökfelt, 2001) such as NTS, PAG (periaqueductal gray), and thalamus, which receive projections from the ArcN and contain significant densities of Y1R and Y5R protein.

The locus coeruleus and subcoeruleus are cell groups that contain intensely labeled cells for both Y1 and Y5 receptors and numerous processes that contain Y5 immunostaining. Because the majority of cells in the LC are noradrenergic, it is likely that NPY receptors are present on catecholaminergic cells. The noradrenergic neurons in the LC colocalize with galanin and NPY (Holets et al., 1988; Moore and Gustafson, 1989; Xu et al., 1998b) and project to several structures, including the forebrain, hippocampus, thalamus, preoptic area, and hindbrain (reviewed in Aston-Jones et al., 1995). The activity of these cells, therefore, is of possible importance to the regulation of several processes, including hormone secretion (Anselmo-Franci et al., 1997), arousal (Aston-Jones et al., 2001), blood pressure (Miyawaki et al., 1991), and anxiety, although these anxiolytic actions are likely due to the activation of Y2 receptors (Kask et al., 1998a). Studies by Yang et al. (1996) showed that Y1R-ir is present within the majority of tyrosine hydroxylase-positive cells of the medullary A1, A2, and C1–3 cell groups, and it is possible, therefore, that noradrenergic cells in the LC may also coexpress NPY receptors, thereby regulating the ability of these neurons to produce and release norepinephrine and NPY.

SUMMARY

The goal of the present studies was to compare the distribution of Y1 and Y5 receptor-ir in the brain with the intent to provide further insight to the cellular distribution of these proteins and regions where they may overlap, perhaps on the same neural substrates. There are several brain regions where the cellular distribution of Y1R- and Y5R-ir are very similar, those being the DBB (Fig. 8), reticular thalamus (Fig. 11), hippocampus (CA2–3, Fig. 7), BLA (Fig. 10), PVN/SON (Fig. 13), locus coeruleus (Fig. 14), Mo5 and Me5 (Fig. 14), and cerebellum. In many other areas, both receptors are present yet their localization within brain nuclei is different. Colocalization of Y1R- and Y5R-ir has been identified in several brain regions, including the cerebral cortex, hippocampus, thalamus, and caudate putamen. As activation of both Y1 and Y5 receptors contribute to the function of several physiological systems, understanding the distribution, function, and regulation of these receptors is an integral part of understanding the role of NPY and its receptors in physiological processes. Using well characterized antibodies can further elucidate the cellular distribution of Y1 and Y5 receptors as well as identify projection sites of NPY receptive neurons.

ACKNOWLEDGMENTS

We thank Joanna Romanelli for her expert technical assistance. Analysis of tissues by using confocal microscopy was made possible through the use of the Microscope and Imaging Facility at Finch University of Health Sciences/The Chicago Medical School.

LITERATURE CITED

Adams JC. 1992. Biotin amplification of biotin and horseradish peroxidase signals in histochemical stains. J Histochem Cytochem 40:1457–1463.

Allen YS, Adrian TE, Allen JM, Tatemoto K, Crow TJ, Bloom SR, Polak JM. 1983. Neuropeptide Y distribution in the rat brain. Science 221: 877–879.

Allen CJ, Ghilardi JR, Vigna SR, Mannon PJ, Taylor IL, McVey DC, Maggio JE, Mantyh PW. 1993. Neuropeptide Y/peptide YY receptor binding sites in the heart: localization and pharmacological characterization. Neuroscience 53:889–898.

Anselmo-Franci JA, Franci CR, Krulich L, Antunes-Rodrigues J, McCann SM. 1997. Locus coeruleus lesions decrease norepinephrine input into the medial preoptic area and medial basal hypothalamus and block the LH, FSH and prolactin preovulatory surge. Brain Res 767:289–296.

Armstrong WE, Scholer J, McNeill TH. 1982. Immunocytochemical, Golgi and electron microscopic characterization of putative dendrites in the ventral glial lamina of the rat supraoptic nucleus. Neuroscience 7:679–694.

Aston-Jones G, Shipley MT, Grzanna R. 1995. The locus coeruleus, A5 and A7 noradrenergic cell groups. In: Paxinos G, editor. The rat nervous system. New York: Academic Press. p 183–206.

Aston-Jones G, Chen S, Zhu Y, Oshinsky ML. 2001. A neural circuit for circadian regulation of arousal. Nat Neurosci 4:732–738.

Baraban SC, Hollopeter G, Erickson JC, Schwartzkroin PA, Palmiter RD. 1997. Knock-out mice reveal a critical antiepileptic role for neuropeptide Y. J Neurosci 17:8927–8936.

Bard JA, Walker MW, Branchek TA, Weinshank RL. 1995. Cloning and functional expression of a human Y4 subtype receptor for pancreatic polypeptide, neuropeptide Y, and peptide YY. J Biol Chem 270:26762–26765.

Bauer-Dantoin AC, McDonald JK, Levine JE. 1991. Neuropeptide Y potentiates luteinizing hormone (LH)-releasing hormone-stimulated LH surges in pentobarbital-blocked proestrous rats. Endocrinology 129: 402–408.

Besecke LM, Levine JE. 1994. Acute increase in responsiveness of luteinizing hormone (LH)- releasing hormone nerve terminals to neuropeptide-Y stimulation before the preovulatory LH surge. Endocrinology 135:63–66.

Besecke LM, Wolfe AM, Pierce ME, Takahashi JS, Levine JE. 1994. Neuropeptide Y stimulates luteinizing hormone-releasing hormone release

from superfused hypothalamic GT1-7 cells. Endocrinology 135:1621–1627.

Biello SM. 1995. Enhanced photic phase shifting after treatment with antiserum to neuropeptide Y. Brain Res 673:25–29.

Broberger C, Hökfelt T. 2001. Hypothalamic and vagal neuropeptide circuitries regulating food intake. Physiol Behav 74:669–682.

Broberger C, Visser TJ, Kuhar MJ, Hokfelt T. 1999. Neuropeptide Y innervation and neuropeptide Y Y1-receptors expressing neurons in the paraventricular hypothalamic nucleus of the mouse. Neuroendocrinology 70:295–305.

Caberlotto L, Tinner B, Bunnemann B, Agnati L, Fuxe K. 1998. On the relationship of neuropeptide Y Y1 receptor-immunoreactive neuronal structures to the neuropeptide Y-immunoreactive nerve terminal networks. A double immunolabelling analysis in the rat brain. Neuroscience 86:827–845.

Campbell RE, ffrench-Mullen JMH, Cowley MA, Smith MS, Grove KL. 2001. Hypothalamic circuitry of neuropeptide Y regulation of neuroendocrine function and food intake via the Y5 receptor subtype. Neuroendocrinology 74:106–119.

Campbell RE, Smith MS, Allen SE, Grayson BE, ffrench-Mullen JMH, Grove KL. 2003. Orexin neurons express a functional pancreatic polypeptide Y4 receptor. J Neurosci 23:1487–1497.

Carter DA, Vallejo M, Lightman SL. 1985. Cardiovascular effects of neuropeptide Y in the nucleus tractus solitarius of rats: relationship with noradrenaline and vasopressin. Peptides 6:421–425.

Chronwall BM. 1989. Anatomical distribution of NPY and NPY messenger RNA in rat brain. In: Mutt V, Hökfelt T, Fuxe K, Lundberg JM, editors. New York: Raven Press. p 51–59.

Chronwall BM, DiMaggio DA, Massari VJ, Pickel VM, Ruggiero DA, O'Donohue TL. 1985. The anatomy of neuropeptide-Y-containing neurons in the rat brain. Neuroscience 15:1159–1181.

de Quidt ME, Emson PC. 1986. Distribution of neuropeptide Y-like immunoreactivity in the rat central nervous system. II. Immunohistochemical analysis. Neuroscience 18:545–618.

Decavel C, Curras MC. 1997. Increased expression of the N-methyl-D-aspartate receptor subunit, NR1, in immunohistochemically identified magnocellular hypothalamic neurons during dehydration. Neuroscience 78:191–202.

Duhault J, Boulanger M, Chamorro S, Boutin JA, Zuana OD, Douillet E, Fauchère JL, Félétou M, Germain M, Husson B, Vega AM, Renard P, Tisserand F. 2000. Food intake regulation in rodents: Y5 or Y1 NPY receptors or both. Can J Physiol Pharmacol 78:173–185.

Dumont Y, Fournier A, St. Pierre S, Quirion R. 1993. Comparative characterization and autoradiographic distribution of neuropeptide Y receptor sites in the rat brain. J Neurosci 13:73–86.

Dumont Y, Fournier A, Quirion R. 1998a. Expression and characterization of the neuropeptide Y Y5 receptor subtype in the rat brain. J Neurosci 18:5565–5574.

Dumont Y, Jacques D, Bouchard P, Quirion R. 1998b. Species differences in the expression and distribution of the neuropeptide Y Y1, Y2, Y4 and Y5 receptors in rodents, guinea pig and primates brains. J Comp Neurol 402:372–384.

Durkin MM, Walker MW, Smith KE, Gustafson EL, Gerald C, Branchek TA. 2000. Expression of a novel neuropeptide Y receptor subtype involved in food intake: an in situ hybridization study of Y5 mRNA distribution in rat brain. Exp Neurol 165:90–100.

Ehlers CL, Somes C, Lopez A, Kirby D, Rivier JE. 1997. Electrophysiological actions of neuropeptide Y and its analogs: new measures for anxiolytic therapy? Neuropsychopharmacology 17:34–43.

Elias CF, Saper CB, Maratos-Flier E, Tritos NA, Lee C, Kelly J, Tatro JB, Hoffman GE, Ollmann MM, Barsh GS, Sakurai T, Yanagisawa M, Elmquist JK. 1998. Chemically defined projections linking the mediobasal hypothalamus and the lateral hypothalamic area. J Comp Neurol 402:442–459.

Eva C, Keinanen K, Monyer H, Seeburg P, Sprengel R. 1990. Molecular cloning of a novel G protein-coupled receptor that may belong to the neuropeptide receptor family. FEBS Lett 271:81–84.

Eva C, Oberto A, Sprengel R, Genazzani E. 1992. The murine NPY-1 receptor gene. Structure and delineation of tissue-specific expression. FEBS Lett 314:285–288.

Everitt BJ, Hökfelt T, Terenius L, Tatemoto K, Mutt V, Goldstein M. 1984. Differential co-existence of neuropeptide Y (NPY)-like immunoreactivity with catecholamines in the central nervous system of the rat. Neuroscience 11:443–462.

Fuxe K, Agnati LF, Aguirre JA, Bjelke B, Tinner B, Merlo Pich E, Eneroth P. 1991. On the existence of volume transmission in the central neuropeptide Y neuronal systems. Studies on transmitter receptor mismatches and on biological effects of neuropeptide Y fragments. In: Fuxe K, Agnati L, editors. Volume transmission in the brain: novel mechanisms for neural transmission. New York: Raven Press, Ltd. p 105–130.

Gehlert DR, Gackenheimer SL. 1997. Differential distribution of neuropeptide Y Y1and Y2 receptors in rat and guinea pig brains. Neuroscience 76:215–224.

Gerald C, Walker MW, Pierre J-J, He C, Branchek TA, Weinshank RL. 1995. Expression cloning and pharmacological characterization of a human hippocampal neuropeptide Y/peptide YY Y2 receptor subtype. J Biol Chem 270:26758–26761.

Gerald C, Walker MW, Criscione L, Gustafson EL, Batzi-Hartmann C, Branchek TA, Weinshank RL. 1996. A receptor subtype involved in neuropeptide-Y-induced food intake. Nature 382:168–171.

Ghilardi JR, Allen CJ, Vigna SR, McVey DC, Mantyh PW. 1994. Cholecystokinin and neuropeptide Y receptors on single rabbit vagal afferent ganglion neurons: site of prejunctional modulation of visceral sensory neurons. Brain Res 633:33–40.

Glass MJ, Chan J, Pickel VM. 2002. Ultrastructural localization of neuropeptide Y Y1 receptors in the rat medial nucleus tractus solitarius: relationships with neuropeptide Y or catecholamine neurons. J Neurosci Res 67:753–765.

Gray TS. 1991. Limbic pathways and neurotransmitters as mediators of autonomic and neuroendocrine responses to stress. In: Brown MR, Koob GF, Rivier C, editors. Stress: neurobiology and neuroendocrinology. New York: Marcel Dekker, Inc. p 73–89.

Gray TS, Bingaman EW. 1996. The amygdala: corticotropin-releasing factor, steroids, and stress. Crit Rev Neurobiol 10:155–168.

Gray TS, Carney MF, Magnuson DJ. 1989. Direct projections from the central amygdaloid nucleus to the hypothalamic paraventricular nucleus: possible role in stress-induced adrenocorticotropin release. Neuroendocrinology 50:433–446.

Grove KL, Campbell RE, ffrench-Mullen JMH, Cowley MA, Smith MS. 2000. Neuropeptide Y Y5 receptor protein in the cortical/limbic system and brainstem of the rat: expression on γ-aminobutyric acid and corticotropin-releasing hormone neurons. Neuroscience 100:731–740.

Guo H, Castro PA, Palmiter RD, Baraban SC. 2002. Y5 receptors mediate neuropeptide Y actions at excitatory synapses in area CA3 of the mouse hippocampus. J Neurophysiol 87:558–566.

Hastings JA, McClure-Sharp JM, Morris MJ. 2001. NPY Y1 receptors exert opposite effects on corticotropin releasing factor and noradrenaline overflow from the rat hypothalamus in vitro. Brain Res 890:32–37.

Heilig M, McLoed S, Brot M, Heinrichs SC, Menzaghi F, Koob GF, Britton KT. 1993. Anxiolytic-like actions of neuropeptide Y: mediation by Y1 receptors in amygdala, and dissociation from food intake effects. Neuropsychopharmacology 8:357–363.

Herzog H, Hort Y, Schneider R, Shine J. 1995. Seminalplasmin: recent evolution of another member of the neuropeptide Y gene family. Proc Natl Acad Sci U S A 92:594–598.

Herzog H, Darby K, Ball H, Hort Y, Beck-Sickinger AG, Shine J. 1997. Overlapping gene structure of the human neuropeptide Y receptor subtypes Y1 and Y5 suggests coordinate transcriptional regulation. Genomics 41:315–319.

Ho MW, Beck-Sickinger AG, Colmers WF. 2000. Neuropeptide Y(5) receptors reduce synaptic excitation in proximal subiculum, but not epileptiform activity in rat hippocampal slices. J Neurophysiol 83:723–734.

Holets VR, Hökfelt T, Rokaeus A, Terenius L, Goldstein M. 1988. Locus coeruleus neurons in the rat containing neuropeptide Y, tyrosine hydroxylase or galanin and their efferent projections to the spinal cord, cerebral cortex and hypothalamus. Neuroscience 24:893–906.

Kalia M, Fuxe K. 1985. Rat medulla oblongata. I. Cytoarchitectonic considerations. J Comp Neurol 233:285–307.

Kalra SP, Fuentes M, Fournier A, Parker SL, Crowley WR. 1992. Involvement of the Y-1 receptor subtype in the regulation of luteinizing hormone secretion by neuropeptide Y in rats. Endocrinology 130:3323–3330.

Kapoor JR, Sladek CD. 2001. Substance P and NPY differentially potentiate ATP and adrenergic stimulated vasopressin and oxytocin release. Am J Physiol 280:R69–R78.

Kask A, Rago L, Harro J. 1998a. Anxiolytic-like effect of neuropeptide Y (NPY) and NPY_{13-36} microinjected into vicinity of locus coeruleus in rats. Brain Res 788:345–348.

Kask A, Rago L, Harro J. 1998b. Evidence for involvement of neuropeptide

Y receptors in the regulation of food intake: studies with Y1-selective antagonist BIBP3226. Br J Pharmacol 124:1507–1515.

Kask A, Harro J, Von Horsten S, Redrobe JP, Dumont Y, Quirion R. 2002. The neurocircuitry and receptor subtypes mediating anxiolytic-like effects of neuropeptide Y. Neurosci Biobehav Rev 26:259–283.

Khanna S, Sibbald JR, Day TA. 1993. Neuropeptide Y modulation of A1 noradrenergic neuron input to supraoptic vasopressin cells. Neurosci Lett 161:60–64.

Kopp J, Xu ZQ, Zhang X, Pedrazzini T, Herzog H, Kresse A, Wong H, Walsh JH, Hökfelt T. 2002. Expression of the neuropeptide Y Y1 receptor in the CNS of rat and of wild-type and Y1 receptor knock-out mice. Focus on immunohistochemical localization. Neuroscience 111: 443–532.

Larhammar D. 1996. Structural diversity of receptors for neuropeptide Y, peptide YY and pancreatic polypeptide. Regul Pept 65:165–174.

Larsen PJ, Mikkelsen JD, Jessop DS, Lightman SL, Chowdrey HS. 1993. Neuropeptide Y mRNA and immunoreactivity in hypothalamus neuroendocrine neurons: effect of adrenalectomy and chronic osmotic stimulation. J Neurosci 13:1138–1147.

Larsen PJ, Jukes KE, Chowdrey HS, Lightman SL, Jessop DS. 1994. Neuropeptide-Y potentiates the secretion of vasopressin from the neurointermediate lobe of the rat pituitary gland. Endocrinology 134: 1635–1639.

Leibowitz SF, Sladek CD, Spencer L, Tempel D. 1988. Neuropeptide Y, epinephrine, norepinephrine in the paraventricular nucleus: stimulation of feeding and the release of corticosterone, vasopressin and glucose. Brain Res Bull 21:905–912.

Leupen SM, Besecke LM, Levine JE. 1997. Neuropeptide Y Y1-receptor stimulation is required for physiological amplification of preovulatory luteinizing hormone surges. Endocrinology 138:2735–2739.

Li C, Chen P, Smith MS. 1999. Morphological evidence for direct interaction between arcuate nucleus neuropeptide Y (NPY) neurons and gonadotropin-releasing hormone neurons and the possible involvement of NPY Y1 receptors. Endocrinology 140:5382–5390.

Liu JP, Clarke IJ, Funder JW, Engler D. 1994. Studies of the secretion of corticotropin-releasing factor and arginine vasopressin into the hypophysial-portal circulation of the conscious sheep. II. The central noradrenergic and neuropeptide Y pathways cause immediate and prolonged hypothalamic-pituitary-adrenal activation. Potential involvement in the pseudo-Cushing's syndrome of endogenous depression and anorexia nervosa. J Clin Invest 93:1439–1450.

Lundberg JM, Terenius L, Hökfelt T, Martling CR, Tatemoto K, Mutt V, Polak J, Bloom S, Goldstein M. 1982. Neuropeptide Y (NPY)-like immunoreactivity in peripheral noradrenergic neurons and effects of NPY on sympathetic function. Acta Physiol Scand 116:477–480.

Marsh DJ, Hollopeter G, Kafer KE, Palmiter RD. 1998. Role of the Y5 neuropeptide Y receptor in feeding and obesity. Nat Med 4:718–721.

Marsh DJ, Baraban SC, Hollopeter G, Palmiter RD. 1999. Role of the Y5 neuropeptide Y receptor in limbic seizures. Proc Natl Acad Sci U S A 96:13518–13523.

Michalkiewicz M, Suzuki M. 1994. Adenohypophyseal vasoactive intestinal peptide and neuropeptide Y responses to hypothyroidism are abolished after anterolateral deafferentation of the hypothalamus. Neuroendocrinology 59:85–91.

Migita K, Loewy AD, Ramabhadran TV, Krause JE, Waters SM. 2001. Immunohistochemical localization of the neuropeptide Y Y1 receptor in rat central nervous system. Brain Res 889:23–37.

Mikkelsen JD, Larsen PJ. 1992. A high concentration of NPY(Y1)-receptor mRNA-expressing cells in the rat arcuate nucleus. Neurosci Lett 148: 195–198.

Miyawaki T, Kawamura H, Komatsu K, Yasugi T. 1991. Chemical stimulation of the locus coeruleus: inhibitory effects on hemodynamics and renal sympathetic nerve activity. Brain Res 568:101–108.

Moore RY, Gustafson EL. 1989. The distribution of dopamine-β-hydroxylase, neuropeptide Y and galanin in locus coeruleus neurons. J Chem Neuroanat 2:95–106.

Naveilhan P, Neveu I, Arenas E, Ernfors P. 1998. Complementary and overlapping expression of Y1, Y2 and Y5 receptors in the developing and adult mouse nervous system. Neuroscience 87:289–302.

Niimi M, Sato M, Taminato T. 2001. Neuropeptide Y in central control of feeding and interactions with orexin and leptin. Endocrine 14:269–273.

Ohkubo T, Niwa M, Yamashita K, Kataoka Y, Shigematsu K. 1990. Neuropeptide Y (NPY) and peptide YY (PYY) receptors in rat brain. Cell Mol Neurobiol 10:539–552.

Parker RMC, Herzog H. 1999. Regional distribution of Y-receptor subtype mRNAs in rat brain. Eur J Neurosci 11:1431–1448.

Paxinos G, Watson C. 1997. The rat brain in stereotaxic coordinates. Orlando, FL: Academic Press, Inc.

Pelletier G, Li S, Hong M, Fournier A, St. Pierre S. 1994. Role of neuropeptide Y in the regulation of gonadotropin releasing hormone (GnRH) gene expression in the rat preoptic area. Mol Brain Res 26:696–673.

Pesold C, Treit D. 1995. The central and basolateral amygdala differentially mediate the anxiolytic effects of benzodiazepines. Brain Res 671:213–221.

Pickel VM, Beck-Sickinger AG, Chan RKW, Wieland HA. 1998. Y1 receptors in the nucleus accumbens: ultrastructural localization and association with neuropeptide Y. J Neurosci Res 52:54–68.

Pronchuk N, Beck-Sickinger AG, Colmers WF. 2002. Multiple NPY receptors inhibit GABA(A) synaptic responses of rat medial parvocellular effector neurons in the hypothalamic paraventricular nucleus. Endocrinology 143:535–543.

Quirion R, Martel J-C, Dumont Y, Cadiuex A, Jolicoeur F, St. Pierre S, Fournier A. 1990. Neuropeptide Y receptors: autoradiographic distribution in the brain and structure-activity relationships. Ann N Y Acad Sci 611:58–72.

Raposinho PD, Broqua P, Pierroz DD, Hayward A, Dumont Y, Quirion R, Junien J-L, Aubert ML. 1999. Evidence that the inhibition of luteinizing hormone secretion exerted by central administration of neuropeptide Y (NPY) in the rat is predominantly mediated by the NPY-Y5 receptor subtype. Endocrinology 140:4046–4066.

Roozendaal B, Koolhaas JM, Bohus B. 1997. The role of the central amygdala in stress and adaption. Acta Physiol Scand 161:51–54.

Ruigrok TJH, Cella F. 1995. Precerebellar nuclei and red nucleus. In: Paxinos G, editor. The rat nervous system. San Diego CA: Academic Press. p 277–308.

Sajdyk TJ, Shekhar A. 1997. Excitatory amino acid receptor antagonists block the cardiovascular and anxiety responses elicited by gamma-aminobutyric acid A receptor blockade in the basolateral amygdala of rats. J Pharmacol Exp Ther 283:969–977.

Sajdyk TJ, Schober DA, Gehlert DR. 2002. Neuropeptide Y receptor subtypes in the basolateral nucleus of the amygdala modulate anxiogenic responses in rats. Neuropharmacol 43:1165–1172.

Sajdyk TJ, Vandergriff MG, Gehlert DR. 1999. Amygdalar neuropeptide Y Y1 receptors mediate the anxiolytic-like actions of neuropeptide Y in the social interaction test. Eur J Pharmacol 368:143–147.

Schaffhauser AO, Stricker-Krongrad A, Brunner L, Cumin F, Gerald C, Whitebread S, Criscione L, Hofbauer KG. 1997. Inhibition of food intake by neuropeptide Y Y5 receptor antisense oligodeoxynucleotides. Diabetes 46:1792–1798.

Stanley BG, Chin AS, Leibowitz SF. 1985. Feeding and drinking elicited by central injection of neuropeptide Y: evidence for a hypothalamic site(s) of action. Brain Res Bull 14:521–524.

Stanley BG, Kyrkouli SE, Lampert S, Leibowitz SF. 1986. Neuropeptide Y chronically injected into the hypothalamus: a powerful neurochemical inducer of hyperphagia and obesity. Peptides 7:1189–1192.

Stanley BG, Magdalin W, Seirafi A, Thomas WJ, Leibowitz SF. 1993. The perifornical area: the major focus of (a) patchily distributed hypothalamic neuropeptide Y-sensitive feeding system(s). Brain Res 604:304–317.

Steinbusch HWM, Niewenhuys R. 1983. The raphe nuclei of the rat brainstem: a cytoarchitectonic and immunohistochemical study. In: Emson P, editor. Chemical neuroanatomy. New York: Raven Press. p 131–207.

Sun QQ, Akk G, Huguenard JR, Prince DA. 2001. Differential regulation of GABA release and neuronal excitability mediated by neuropeptide Y1 and Y2 receptor in rat thalamic neurons. J Physiol 531:81–94.

Urban JH, Das I, Levine JE. 1996. Steroid modulation of neuropeptide Y-induced luteinizing hormone releasing hormone release from median eminence fragments from male rats. Neuroendocrinology 63:112–119.

Wahlestedt C, Pich EM, Koob GF, Yee F, Heilig M. 1993. Modulation of anxiety and neuropeptide Y-Y1 receptors by antisense oligodeoxynucleotides. Science 259:528–531.

Wahlestedt C, Skagerberg G, Ekman R, Heilig M, Sundler F, Hakanson R. 1987. Neuropeptide Y (NPY) in the area of the hypothalamic paraventricular nucleus activates the pituitary-adrenocortical axis in the rat. Brain Res 417:33–38.

Widdowson PS. 1997. Regionally selective down-regulation of NPY recep-

tor subtypes in the obese Zucker rat. Relationship to the Y5 "feeding" receptor. Brain Res 758:17–25.

Xu B, Kalra PS, Moldawer LL, Kalra SP. 1998a. Increased appetite augments hypothalamic NPY Y1 receptor gene expression: effects of anorexigenic ciliary neurotropic factor. Regul Pept 75–76:391–395.

Xu ZQ, Shi TJ, Hökfelt T. 1998b. Galanin/GMAP- and NPY-like immunoreactivities in locus coeruleus and noradrenergic nerve terminals in the hippocampal formation and cortex with notes on the galanin-R1 and -R2 receptors. J Comp Neurol 392:227–251.

Yang S-N, Bunnemann B, Cintra A, Fuxe K. 1996. Localization of neuropeptide Y Y1 receptor-like immunoreactivity in catecholaminergic neurons of the rat medulla oblongata. Neuroscience 73:519–530.

Yokosuka M, Kalra PS, Kalra SP. 1999. Inhibition of neuropeptide Y (NPY)-induced feeding and cfos response in magnocellular paraventricular nucleus by a NPY receptor antagonist: a site of NPY action. Endocrinology 140:4494–4500.

Zhang X, Bao L, Xu ZQ, Kopp J, Arvidsson U, Elde R, Hökfelt T. 1994. Localization of neuropeptide Y Y1 receptors in the rat nervous system with special reference to somatic receptors on small dorsal root ganglion neurons. Proc Natl Acad Sci U S A 91:11738–11742.